
Electronic Thesis and Dissertation Repository

9-23-2019 10:00 AM

Determining the Relative Transmission Fitness of HIV-1 Subtypes A, B, C, and D

Spencer Yeung, *The University of Western Ontario*

Supervisor: Arts, Eric J., *The University of Western Ontario*

Co-Supervisor: Prodger, Jessica L., *The University of Western Ontario*

A thesis submitted in partial fulfillment of the requirements for the Master of Science degree in Microbiology and Immunology

© Spencer Yeung 2019

Follow this and additional works at: <https://ir.lib.uwo.ca/etd>



Part of the [Immune System Diseases Commons](#), [Pathological Conditions, Signs and Symptoms Commons](#), [Virology Commons](#), and the [Virus Diseases Commons](#)

Recommended Citation

Yeung, Spencer, "Determining the Relative Transmission Fitness of HIV-1 Subtypes A, B, C, and D" (2019). *Electronic Thesis and Dissertation Repository*. 6683.
<https://ir.lib.uwo.ca/etd/6683>

This Dissertation/Thesis is brought to you for free and open access by Scholarship@Western. It has been accepted for inclusion in Electronic Thesis and Dissertation Repository by an authorized administrator of Scholarship@Western. For more information, please contact wlsadmin@uwo.ca.

Abstract

There is *in vivo* evidence that suggests the genetic diversity of HIV-1 subtypes influence heterosexual transmission efficiency. To recapitulate sexual transmission *in vitro*, blocks of genital tissue were exposed to mixtures of genetically different subtype viruses. Migrating immune cells were collected and co-cultured with a CD4+ T-cell line permissive to HIV infection (PM1) to measure dendritic cell virus transfer; HIV-exposed tissues were cultured separately. Next generation sequencing (NGS) of HIV-1 DNA was used to quantify relative infection rates of the various challenge viruses, and to assess fitness differences in infection of the tissue vs. migratory/T cell co-cultures. Our results suggest a HIV-1 subtype's ability to replicate in susceptible T cells may be predictive of its ability to replicate in susceptible tissue-resident cell populations. However, this may not reflect the ability of a subtype to be transported out of the tissue for infection elsewhere in the body.

Keywords

HIV-1, group M subtypes, disease progression, pathogenic fitness, replicative fitness, transmission fitness

Summary for Lay Audience

Human Immunodeficiency Virus Type 1 (HIV-1) is the causative agent for AIDS. Since the start of the epidemic, HIV-1 has evolved rapidly and resulted in different subtypes that are genetically diverse from one another. These subtypes are what's driving the number of new infections worldwide. Studies have shown that the genetic diversity of the different subtypes contribute to how fast someone will start to experience AIDS. In particular, HIV-1 subtype C results in individuals progressing to AIDS at a much slower rate compared to HIV-1 subtypes A, B, and D. Researchers have speculated that this slower disease progression may result in more opportunity for new infections due to the fact that these individuals will likely only seek treatment when they experience AIDS-like symptoms. This makes sense, as HIV-1 subtype C accounts for greater than 50% of infections worldwide when compared to the other subtypes. Although increased opportunity for infection would account for this larger prevalence, the transmission efficiency of the different subtypes may also play a role. To investigate the transmission efficiencies of the different subtypes, I infected explants of genital tissue with these different subtypes and measured their abilities to infect tissue and transmit to susceptible cells. In this study, I found that the ability of a virus to cause disease progression may be able to predict its ability to replicate in the tissue itself. However, this may not relate to the ability of a virus to transmit and infect other parts of the body. Future studies will need to include more viruses to help further discern the differences in transmission efficiencies between the HIV-1 subtypes.

Co-Authorship Statement

Studies presented in this thesis were completed by Spencer Yeung with the assistance of past and present members in the laboratories of Dr. Eric Arts and Dr. Jessica Prodger, and collaborators as listed:

Dr. Immaculate Nankya performed the cloning of acute *env* sequences into the pREC_nfl_{NL4-3}Δenv backbone.

Dr. Dean Elterman provided foreskin tissues from adult men (>18) undergoing elective circumcision at the University Urology Associates (UUA) clinic in Toronto.

Dr. Nicholas Hathaway and Dr. Jeff Bailey at Brown University conducted sequence analyses through their SeekDeep platform.

Acknowledgements

I would like to thank all the members of the Arts/Mann/Gao/Troyer lab, past and present, for supporting me and creating a community of learning and personal growth. The memories I've made with you will last a lifetime and the challenges we've faced together will continually provide me with lessons for my future career endeavours. I would also like to thank the Prodger lab for always pushing me to think outside of the box and giving me the opportunity to work with such diverse minds and personalities. In particular, I'd like to thank my best friend Adam Meadows for teaching me everything I know. Without you, nothing in these past two years would have been possible. You made every experiment fun and every memory priceless.

To Dr. Katja Klein, thank you for your support and guidance during my time here. You were an expert in the explant assay and you showed it!

To my advisory committee, Dr. Jeremy Burton and Dr. Kelly Summers, thank you. Jeremy, I've always admired your industry background and you brought such a fresh outlook to every problem. Kelly, your reputation precedes you. Your ability to build rapport and to provide guidance was spectacular. Thanks to you both.

To my supervisor Dr. Eric Arts, thank you for accepting me into your lab and seeing potential in me. You inspired me to pursue research and taught me the value of seeing the big picture. I strive to possess your vision and perspective.

To my supervisor Dr. Jessica Prodger, thank you from the bottom of my heart. Your ability to empower others is unmatched and your thirst for knowledge is electrifying. As your first

student, I hope I made you proud. Your patience and understanding did not go unnoticed through my many trials and tribulations. I cannot wait to see the things you will achieve in the future!

Table of Contents

ABSTRACT	II
SUMMARY FOR LAY AUDIENCE	III
CO-AUTHORSHIP STATEMENT	IV
ACKNOWLEDGEMENTS	V
TABLE OF CONTENTS	VII
LIST OF TABLES	X
LIST OF FIGURES	XI
LIST OF ABBREVIATIONS	XIII
CHAPTER 1: INTRODUCTION	1
1.1 HIV-1 EPIDEMIC	1
1.2. HIV-1 LIFE CYCLE.....	3
1.3 HIV-1 GENETIC DIVERSITY	5
1.4. HIV-1 INFECTION IN GENITAL TISSUE	5
<i>1.4.1 HIV-1 Infection in Male Genital Tract</i>	8
1.5 HIV-1 TRANSMISSION FITNESS MAY BE DIFFERENT THAN HIV-1 PATHOGENIC FITNESS.....	10
<i>1.5.1. HIV-1 Transmission Bottleneck</i>	10
<i>1.5.2 Rationale for Possible Attenuation of HIV-1 group M viruses</i>	13
1.6 SUBTYPES AND PATHOGENIC FITNESS DIFFERENCES	14
1.7 SUBTYPES AND TRANSMISSION FITNESS DIFFERENCES	16

1.8 HYPOTHESIS AND AIMS	18
CHAPTER 2: MATERIALS AND METHODS	19
2.1 CELLS	19
2.2 VIRUS CLONING AND PROPAGATION	19
2.3 VIRUS QUANTIFICATION	23
2.4 RNA EXTRACTION AND RT-PCR FOR DNA SEQUENCING AND SUBTYPING	24
2.5 <i>EX VIVO</i> TISSUE EXPLANT ASSAY	27
2.6 DIRECT COMPETITIONS ON PM1 CELLS	31
2.7 DNA EXTRACTION AND PCR AMPLIFICATION	31
2.8 NEXT-GENERATION SEQUENCING LIBRARY PREPARATION AND SEQUENCING	34
2.9 SEQUENCE AND STATISTICAL ANALYSIS	37
2.10 QUANTITATIVE POLYMERASE CHAIN REACTION (QPCR)	37
CHAPTER 3: RESULTS	39
3.1 VIRUS QUANTIFICATION AND TITRES	39
3.2 SUBTYPE CONFIRMATION	42
3.3 DIRECT COMPETITIONS ON PM1 CELLS TO ASSESS REPLICATIVE FITNESS	44
3.4 MULTI-VIRUS COMPETITIONS IN HUMAN EXPLANT TISSUE TO ASSESS RELATIVE TRANSMISSION FITNESS	47
3.4.1 USING A LOW MOI MAY RESULT IN STOCHASTIC INFECTION EVENTS THAT DO NOT REFLECT DIFFERENCES IN TRANSMISSION FITNESS BETWEEN SUBTYPES	48
3.4.2 <i>Subtype Transmission Fitness Differences in Cervical Tissue</i>	55
3.4.3 <i>Subtype Transmission Fitness Differences in Foreskin Tissue</i>	60

3.5 RELATIVE ABUNDANCE OF EACH INDIVIDUAL VIRUS IN CERVICAL AND FORESKIN TISSUE	64
CHAPTER 4: DISCUSSION AND CONCLUSION	68
REFERENCES.....	74
CURRICULUM VITAE.....	81

List of Tables

Table 1. Acute env chimeric viruses used in this study	21
Table 2. DNA Primers used in this study.....	26
Table 3. Acute env chimeric viruses included in each competition.....	30
Table 4. Viral titres calculated using the Reed-Muench Method, corresponding to positive signals in phosphor images.....	41

List of Figures

Figure 1. HIV-1 Structure	4
Figure 2. Schematic of HIV-1 transmission in the cervix	9
Figure 3. Schematic of PCR amplification of HIV-1 env and cloning into pREC_nfl_{NL4-3}Δenv/URA3 (courtesy of Dr. Eric Arts)	22
Figure 4. Example of RT Assay protocol, quantifying four viruses	25
Figure 5. Experimental protocol for the ex vivo explant assay	29
Figure 6. PCR strategy for Next-Generation Sequencing	33
Figure 7. NGS preparation and sequence analysis pipeline	36
Figure 8. Phosphor Images produced from RT assay of each virus used in the study	40
Figure 9. Phylogenetic alignment for subtype identification of each env chimeric virus	43
Figure 10. Average relative abundance of each subtype in PM1 cells	45
Figure 11. Individual multi-virus competitions performed on PM1 cells, grouped by subtypes	46
Figure 12. Average relative abundance of each subtype in cervical tissue and from migratory cells after infection at 0.01MOI	50
Figure 13. Individual multi-virus competitions using cervical tissue at 0.01 MOI, grouped by subtype	51
Figure 14. Two representative electrophoresis gels to demonstrate PCR efficiencies	53

Figure 15. Comparison of absolute quantity of integrated HIV DNA in tissue between MOI conditions.....	54
Figure 16. Average relative abundance of each subtype in cervical tissue and from migratory cells after infection at 0.05 MOI.....	57
Figure 17. Individual multi-virus competitions using cervical tissue at 0.05 MOI, grouped by subtype.....	58
Figure 18. Average relative abundance of each subtype in foreskin tissue and from migratory cells after infection at 0.05 MOI.....	61
Figure 19. Individual multi-virus competitions using foreskin tissue at 0.05 MOI, grouped by subtype.....	62
Figure 20. Average relative abundance of each individual virus in cervical tissue at 0.05 MOI.....	66
Figure 21. Average relative abundance of each individual virus in foreskin tissue at 0.05 MOI.....	67

List of Abbreviations

AIDS	Acquired Immunodeficiency Syndrome
ART	Antiretroviral Therapy
bNAbs	Broadly Neutralizing Antibodies
CCR5	C-C Chemokine Receptor type 5
CD4	Cluster of Differentiation 4
CHAVI	Center of HIV/AIDS Vaccine Immunology
CRF	Circulating Recombinant Forms
CXCR4	C-X-C Chemokine Receptor Type 4
DEAE-C	Diethylaminoethyl Cellulose
DC	Dendritic Cells
DNA	Deoxyribonucleic acid
FBS	Fetal Bovine Serum
FRT	Female Reproductive Tract
GFP-Vpr	Green Fluorescent Protein-Vpr
GP120	Glycoprotein 120
HIV	Human Immunodeficiency Virus
IU	Infectious Units
LC	Langerhans Cells
MOI	Multiplicity of Infection
MSM	Men who have Sex with Men
NDRI	National Disease Research Interchange
NGS	Next Generation Sequencing
NIH	National Institutes of Health
PCR	Polymerase Chain Reaction
PBMCs	Peripheral Blood Mononuclear Cells
qPCR	Quantitative Polymerase Chain Reaction
TCID	Tissue Culture Infectious Dose
T/F	Transmitted/Founder
RNA	Ribonucleic Acid
RT	Reverse Transcription
RT-PCR	Reverse Transcription Polymerase Chain Reaction
SSC	Saline-Sodium Citrate Buffer
UUA	University Urology Associates
UNAIDS	The Joint United Nations Programme on HIV and AIDS (UNAIDS)
WHO	World Health Organization

Chapter 1: Introduction

1.1 HIV-1 Epidemic

Human Immunodeficiency Virus type 1 (HIV-1), the causative agent for Acquired Immunodeficiency Syndrome (AIDS), was first isolated from a patient in 1983^{1,2}. As time has passed, HIV-1 has become a significant challenge to public and global health and continues to challenge populations due to the high frequency of undiagnosed infections, a disproportionate effect on marginalized populations, and the absence of compliance-free preventative measures and a cure. In 2018, there were 37.9 million people living with HIV/AIDS worldwide which is irrespective of the fact that 74.9 million people have been infected with HIV-1 since its discovery³. The effect on the human species is staggering, with over 35 million losing their life to the battle against HIV/AIDS⁴. Despite a vast number of ongoing efforts, 1.7 million people worldwide were newly infected with HIV-1 in 2018³ which translates to 3 new infections per minute.

In 2018, 770,000 people died as a result of HIV/AIDS³. This can be seen as an improvement when compared to an astounding 2 million people dying due to AIDS-related deaths in 2008³. A large part in this reduction of mortality can be attributed to the United Nations AIDS Program (UNAIDS) 90-90-90 initiative³. This initiative put forth 3 goals: 90% of individuals living with HIV know their status, of those individuals 90% of them are on antiretroviral (ART) therapy, and 90% of those individuals receiving ART therapy achieve viral suppression. As of 2018, UNAIDS estimated that 79% of people living with HIV know their status, of those 78% were receiving ART, and 86% of those achieved viral

suppression³. The trends are in the right direction, but there is still a lot of work to be done to achieve the 90-90-90 goals.

Different areas of the world are affected by the HIV-1 epidemic in different ways. Sub-Saharan Africa accounts for approximately 70% of individuals living with HIV-1 which translates to an adult prevalence of approximately 4.1%⁴. As a comparison, every other WHO region has a prevalence of less than 1%. For example, the Americas are the next highest, with an adult prevalence of 0.5%. Even within Africa, there are differences in burden of disease. South Africa has an estimated prevalence of 19.2% and is the country with the largest population of individuals living with HIV-1. In contrast, the prevalence of HIV-1 in Senegal is around 0.5%⁴. For new infections globally, heterosexual transmission has been reported to account for 70% of newly acquired infections⁵. The remainder of newly acquired infections can be attributed to other major routes of transmission. These include men who have sex with men (MSM), maternal-infant infection, and injection drug use³. Although heterosexual transmission accounts for the majority of newly acquired infections, the transmission probability per exposure event for men and women are low, ranging from 1 in 700 to 1 in 3000 and 1 in 200 to 1 in 2000, respectively⁵. With heterosexual intercourse being the major route of transmission in Sub-Saharan Africa, women account for approximately 58% of individuals living with HIV-1 in Sub-Saharan Africa⁶. Consequently, decreasing heterosexual transmission of HIV-1 will be an important step towards remedying the number of new infections and mitigating the HIV-1 disease burden across the world.

1.2. HIV-1 Life Cycle

To understand how HIV-1 has impacted so many lives, it is important to understand its life cycle in the human host. The intricacies of HIV-1 replication in human cells provide the basis for vaccine designs and cure strategies; the details of HIV-1 replication in susceptible human cells are well established⁷ and will be detailed here. A direct interaction of HIV-1's *envelope* protein, gp120 (**Figure 1**), and the CD4 receptor on human immune cells is one requirement for infection. However, this interaction is not sufficient to begin entry into cells and one of two chemokine receptors, CCR5 and CXCR4, are also required for this process. In general, certain HIV-1 viruses preferentially bind to CCR5 or CXCR4. Once binding of CD4 and one of CCR5 or CXCR4 occurs, fusion of the HIV-1 envelope and the host cell membrane begins, culminating in the release of the viral capsid (**Figure 1**) into the cytoplasm. Reverse transcription inside the capsid initiates, with HIV-1's native reverse transcriptase introducing a plethora of DNA replication errors in the process of creating double stranded DNA (dsDNA) from its own RNA genome. This high error rate in reverse transcription is the main reason cure and vaccine strategies have been so difficult – HIV-1 evolves very rapidly. Shortly, the dsDNA is transported into the nucleus for integration into the host genome via HIV-1's integrase protein. After this point the integrated DNA, or proviral DNA, utilizes host cell transcription machinery and mRNA transcripts are generated. These RNA molecules are then translated to produce all the necessary structural and enzymatic proteins of HIV-1 leading to budding and release of new HIV-1 particles.

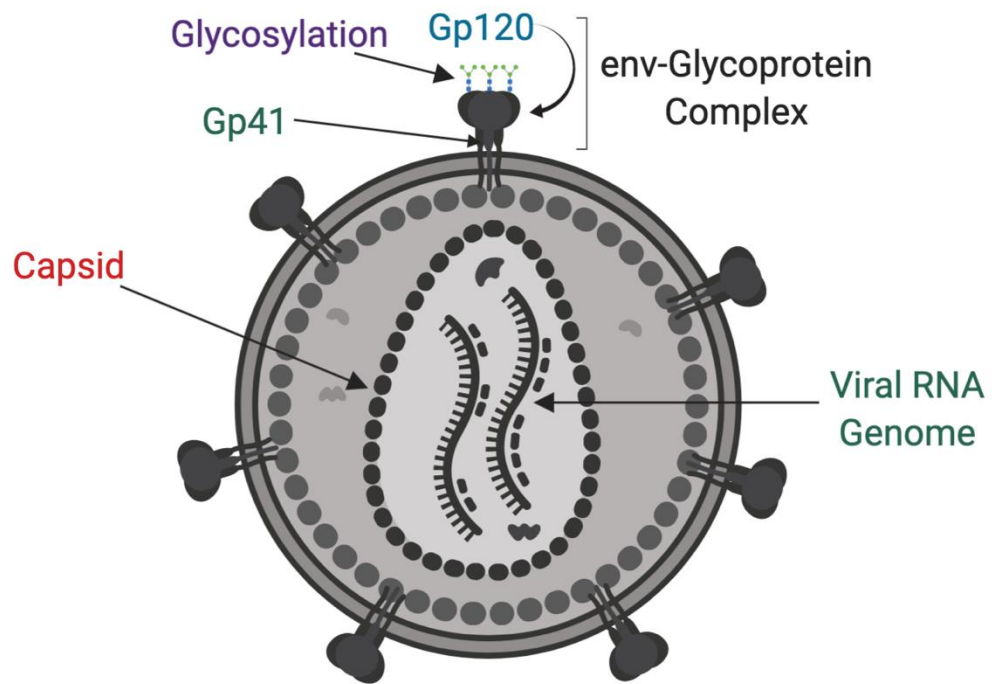


Figure 1. HIV-1 Structure

Different components of HIV-1 involved in HIV-1 infection, transmission, and replication. Gp120, the only surface exposed protein on HIV-1, is an important component of the HIV-1 *envelope* involved in infection and transmission. It is involved in the first interaction between HIV-1 and CD4⁺ T cells. The capsid houses the viral RNA genome.

1.3 HIV-1 Genetic Diversity

Since its discovery, the evolutionary history of HIV-1 and its relation to the epidemic has been of particular interest in the field. HIV-1 accounts for over 98% of infections and is the main driver of new infections and AIDS-related disease worldwide⁸. It has established itself as the primary HIV type for research and treatment efforts. Within HIV-1 there are three lineages: the main (M) group, the new (N) group, and the outlier (O) group^{9,10}. Group M dominates the other groups in its prevalence¹¹, and researchers speculate that a single transmission of HIV-1 from group M coincided with the expansion of the epidemic¹⁰. Over time, divergent evolution of HIV-1 group M has resulted in distinct and diverse subtypes; these subtypes are: A, B, C, D, F, G, H, J, and K and they are also not distributed evenly worldwide⁷. HIV-1 subtypes A, B, and D account for 12%, 10%, and 3% of infections worldwide¹², respectively, while ‘pure’ subtype C or HIV-1 recombinant forms with the *envelope* gene of subtype C are responsible for greater than 50% of the HIV-1 infections worldwide¹². Recombination can occur when an infected cell has two different proviruses¹³. Thus if both transcripts are encapsulated into a virion, the reverse transcriptase can jump between the two templates creating a newly synthesized DNA sequence that is recombinant. Currently, there are 98 known circulating recombinant forms of HIV¹⁴. Taken together, the investigation of HIV-1 group M and the different dominant subtypes is important to attempt to decrease the number of new infections. Transmission of HIV-1 is multi-faceted and involves multiple considerations.

1.4. HIV-1 Infection in Genital Tissue

HIV-1 preferentially replicates and propagates in CD4+ T cells in the mucosa, submucosa, draining lymphatics, and systemic lymphatic tissues¹⁵. One of the most important, if not

the most important factor for predicting HIV-1 infection after exposure is plasma viral load (vL) of the infecting partner¹⁶⁻¹⁸. For HIV-1 discordant monogamous couples, individuals with plasma levels <400 HIV RNA copies/mL did not transmit to their partners^{19,20}. Additional studies investigated the effect of viral load on transmission risk and it was determined that for every log increase in viral load the risk of transmission increased by a factor of 2.45¹⁸.

Using virions labelled with a photoactivatable GFP-Vpr (PA-GFP), Ann M. Carias and her colleagues proposed a model of how HIV-1 interacts with the female reproductive tract (FRT)²¹. When the epithelia of the FRT is intact, HIV-1 virions rarely penetrate and even more rarely into areas with potential target cells. When cellular junctions are absent or degraded, or when the epithelium loses its integrity, virions can readily penetrate the FRT (**Figure 2A**). As a result, virions have a greater chance of interacting with resident intraepithelial Langerhans Cells (LCs) and other susceptible cells. Inflammation of the FRT has also been shown to increase the odds of HIV-1 interacting with target cells in the mucosa²²⁻²⁶. The recruitment of susceptible cells to the FRT alongside mechanisms such as cell junction degradation can all increase the likelihood of HIV-1 transmitting. Carias and colleagues were also able to extrapolate and estimate the number of virions that penetrate the lower FRT per coital act. They estimated that when the acutely-infected donor deposits their viral population into the recipient, potentially 1.49×10^4 virions penetrate the squamous epithelium of the ectocervix per coital act. For the endocervix, they estimate a potential 3.40×10^3 penetrates the simple columnar epithelium.

The specific cell types that HIV-1 infect after exposure in the mucosa are CD4+ T cells, dendritic cells (DCs), or macrophages^{27,28}. As briefly mentioned before, in foreskin²⁹ and cervix³⁰ activated CD4+ T cells and immature Langerhans cells²⁷ are distributed throughout the tissue and susceptible to infection. It is heavily debated whether cell-free virus or cell-associated virus is responsible for sexual transmission and systemic infection³¹⁻³³. However, *in vitro* studies have shown that cell-associated HIV-1 transmission is much more efficient, likely because of concentrated production at intercellular contact points, directional secretion through specialized intercellular synapses, and possibly decreased vulnerability of the virus to host restriction factors and antiviral factors in the environment during transmission³⁴⁻⁴⁰. In general, dendritic cells are involved in the uptake and processing of antigens. *Trans*-infection has been described as a process where dendritic cells will transport the transmitted virus into areas such as the lymphoid tissue and present the virus, resulting in infection of susceptible T cells⁴¹. To demonstrate this, a study used vaginal explant tissue infected with HIV-1 and showed that transmitted viruses bound to DCs, DCs transported them through the mucosa, and subsequently presented HIV-1 to T cells⁴² (**Figure 2B**). Other studies have also shown the ability of epidermal Langerhans cells and dermal DC-SIGN+ dendritic cells to bind infectious viral particles and present them to T cells⁴³⁻⁴⁵. Furthermore, when cervical explant tissue was inoculated with HIV-1, significant *trans* infectivity was detected with budding of virions in DCs harvested from supernatant^{19,20}. Overall, cell-to-cell HIV-1 transmission is an important process and dendritic cells seem to play a critical role in the presentation of HIV-1 viruses to T cells, either in the mucosa or in lymphoid tissue.

The investigation of cell-free HIV-1 transmission is also important, as CD4+ T cells are present in the lamina propria of the vagina, ectocervix, and endocervix and CD4 plays an important role in the infection of T cells. Studies have shown HIV-1 poorly infects cells expressing CCR5 with low levels of CD4⁴⁶⁻⁴⁸. Moreover, models of SIV transmission have shown that the number of mucosal CD4+/CCR5+ T cells is a key determinant of HIV-1 acquisition risk⁴⁸. Overall, HIV-1 is very effective at targeting and infecting CD4+ T cells in the mucosa^{28,49,50} (**Figure 2C**).

1.4.1 HIV-1 Infection in Male Genital Tract

Most of our knowledge about heterosexual transmission of HIV-1 comes from studies done in women. However, studies in men have supported the well-documented findings in women that have already been discussed here. In circumcision studies, it was determined that male circumcision reduces HIV-1 infection in heterosexual men by 60%⁵¹. This suggests that foreskin is the major site of HIV-1 infection in men. In the foreskin, there are many susceptible cells, such as Th17 cells, present for HIV-1 infection⁵². These CD4+ cells express high levels of CCR5 and have enhanced *in vitro* HIV-1 susceptibility^{53,54}. Moreover, *trans*-infection by dendritic cells have been observed through *in vitro* infections of the inner foreskin⁵⁵. In short, many of the mechanisms described in women are most likely to occur in the male genital tract as well, with foreskin being the primary anatomical site for infection⁵⁶⁻⁵⁸.

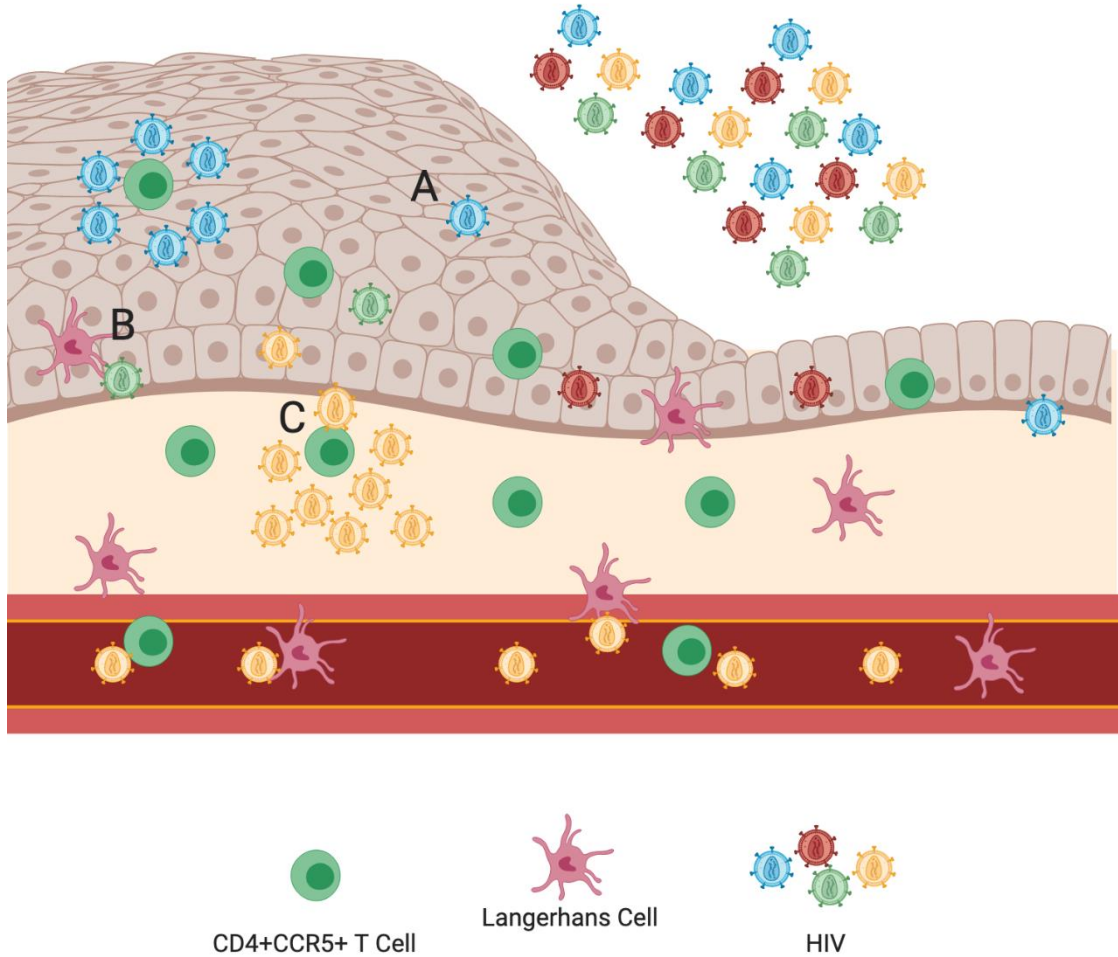


Figure 2. Schematic of HIV-1 transmission in the cervix

A diverse population of HIV-1 is deposited into the uninfected individual. **(A)** When the epithelium loses its integrity, HIV-1 virions can penetrate the epithelium and interact with susceptible cells. **(B)** *Trans*-infection can occur, where tissue resident Langerhans cells can bind to HIV-1 and transport them to areas with susceptible CD4+CCR5+ T cells. **(C)** Even still, HIV-1 is efficient at targeting and infecting CD4+CCR5+ T cells in the tissue.

1.5 HIV-1 Transmission Fitness may be different than HIV-1 Pathogenic Fitness

1.5.1. HIV-1 Transmission Bottleneck

Although the HIV-1 infected donor deposits a diverse viral population into the recipient during sexual intercourse, the majority of the time only 1 single viral variant penetrates the mucosal barrier and establishes systemic infection. In fact, this phenomenon occurs in approximately 80% of heterosexual transmission cases^{59,60}. Termed the “transmission bottleneck”, it is still not very well understood. It should be noted that the narrowing of the viral population can occur in both the donor and the recipient as well as in different anatomical compartments. For example, there is evidence to suggest that the viral population present in the infected donor’s blood is different than the viral population in the same individual’s genital tract^{61–64}. More specifically, it is argued that the viruses in the genital tract are under different selective pressures than those in the blood. However, the focus here will be on the bottleneck that occurs in the recipient mucosa, which is where the most severe bottleneck occurs during transmission⁶⁵.

Shortly after infection, the newly infected host will have a mostly homogenous viral variant population present in their blood⁶⁶. This viral variant is termed the transmitted/founder (T/F) virus and will start to evolve as viral replication occurs. Consistent with this, a more diverse viral population is observed in the blood of a host that has reached chronic infection. The cycle continues if the host remains untreated, where a single viral variant is transmitted from a diverse viral population to an uninfected individual. Building upon this idea, Dr. Katja Klein and her colleagues sought to characterize the sequence diversity of HIV-1

during early infection between two compartments: the female reproductive tract (FRT) and the blood⁶⁷. They compared the intra-patient diversity of the C2-V3 *env* region (gp120) between matched cervical and blood samples from 72 women recruited from Uganda and Zimbabwe. Their findings showed that within seven months of being diagnosed of HIV-1 infection, there was higher HIV-1 *env* diversity in the genital tract compared to the plasma of these patients. This study further showcases that in spite of a diverse viral population being deposited during sexual transmission, when systemic infection is first established it is characterized by a more homogenous viral population.

It is heavily debated whether the HIV-1 bottleneck is due to stochastic events or whether there are actually selective pressures present that dictate the phenotype of the virus that is transmitted. It was first discovered that HIV-1 targeted CD4+ T cells that expressed CCR5 or CXCR4 co-receptors for use of entry into the cell⁶⁸. However, in the majority of cases the virus that is sexually transmitted is homogenous^{66,69} and preferentially uses CCR5 as a co-receptor⁷⁰. Through observations of individuals who lack a functional gene for the CCR5 receptor, these specific individuals were completely resistant to acquiring HIV-1 through sexual transmission⁷¹. This suggests that all of sexual transmission occurs through viruses using CCR5 as a co-receptor. This is contrasted with transmission of HIV-1 through blood, where viruses that preferentially use CXCR4 can also be transmitted⁶⁵. This may mean there are different and unique viral characteristics that are needed for fitness in the tissue vs. the blood.

In addition to the exclusive use of CCR5, T/F *envelopes* have been shown to have shorter surface-exposed variable loops (gp120), fewer N-linked glycosylation sites, and more

sialylation in comparison to chronic viruses⁷²⁻⁷⁴. This is in contrast to characteristics of viruses that allow it to evade broadly neutralizing antibodies (bNAbs). It seems that only once infection occurs, the virus mutates and gains the ability to evade bNAbs by increasing the length of variable loops, adding N-linked glycosylation sites, and altering the composition of the persistent high mannose patch of gp120 subunits⁷⁵⁻⁷⁷. These changes help evade immune pressure, allowing for the repeated infection and killing of CD4+ T cells. Altogether, this suggests that genetic differences between HIV-1 variants can confer differences in transmission fitness. But more importantly, the phenotype of the T/F virus that offers a greater fitness advantage in transmission may or may not offer the same fitness advantage for pathogenicity.

1.5.3 Differences in defining HIV-1 Pathogenic and Transmission fitness

Individuals infected with replication-defective, *nef*-mutated virus demonstrate that individuals infected with a virus that has poor replicative fitness progresses to AIDS-related disease at a slower rate⁷⁸⁻⁸⁰. Moreover, the ability of a virus to replicate in peripheral blood mononuclear cells (PBMCs) has been shown to correlate with decreasing CD4+ cell counts and increasing viral load during disease⁸¹. Thus, the replicative or *pathogenic* fitness of a virus strain can be defined as the relative *ex vivo* replication capacity of HIV-1 in CD4+ T cells and PBMCs⁸²⁻⁸⁴. In contrast, the *ex vivo* transmission fitness of a virus used to be measured by competing HIV-1 isolates in cells of the dendritic lineage, which are derived from blood monocytes or human skin^{27,85}. However more recently, studies have begun to employ genital explant tissue to define transmission fitness^{55,86}. Thus, the *ex vivo* transmission fitness of a virus can be defined by its ability to penetrate genital explant

tissue, infect tissue-resident susceptible cell populations, and bind to resident cells that migrate out of the mucosal layer for *trans*-infection in susceptible T cells.

1.5.2 Rationale for Possible Attenuation of HIV-1 group M viruses

Both opportunity for infection and transmission efficiency are key factors of pathogen survival⁸⁷. As mentioned above, *env* characteristics of the T/F virus may not confer a fitness advantage in evading the immune system. One factor that's important in considering a pathogen's ability to cause disease is its ability to evade the immune system. Thus the T/F virus, the most efficiently transmitted virus, would be anticipated to be less virulent. However, this decreased virulence would theoretically allow more opportunities to transmit to uninfected individuals. At the population-level, a virus' ability to transmit efficiently and have a greater number of opportunities to infect new hosts would allow it to survive in the epidemic at a greater capacity.

For an individual who does not have knowledge of their infection, especially during the acute/early phase of their infection where viral load is the highest, the number of sexual contacts/encounters directly relates to opportunities for HIV-1 infection in uninfected individuals⁸⁸. However, in a population where the number of sexual contacts are decreased, the period of infection with the highest viral load may be recovered by periods of longer asymptomatic infection with a more moderate viral load. In other words, individuals with a more moderate viral load may have more sexual contacts with uninfected individuals over a longer period of time. While high viral load relates to increased opportunity for new infections, a lower HIV-1 virulence could lead to longer periods of asymptomatic disease which could also relate to increased opportunities for new HIV-1 infections. There has

been a disproportionate expansion of HIV-1 subtype C compared to the other dominant group M subtypes. Attempts to define the relative pathogenic and transmission fitness' between the different group M subtypes have been undertaken in hopes of understanding the differential prevalence around the world. The exceptional genetic diversity between the group M subtypes could potentially translate to fitness differences.

1.6 Subtypes and Pathogenic Fitness Differences

To determine the relative pathogenic fitness' of the different HIV-1 group M subtypes, competition experiments involving the different group M subtypes have been widely performed. Employing eight HIV-2, six HIV-1 group O, and 15 group M isolates, pairwise competitions in PBMCs were performed to determine differences in pathogenic fitness⁸⁹. Aside from HIV-2 and HIV-1 group O viruses having the lowest fitness, HIV-1 subtype C was less fit than subtypes A, B, D and CRF01_AE⁸⁹. Further competition experiments showed that when HIV-1 subtype C was competed directly against other dominant group M subtypes, it was at least 100-fold less fit⁸². These pairwise competitions helped to reveal a general fitness order, where HIV-1 subtype B and D were slightly more fit than subtype A and dramatically more fit than subtype C⁸¹.

Perhaps the most convincing form of evidence comes from a recent study by Venner and colleagues⁹⁰. Using a long-term natural history cohort of HIV-1 infected women in Uganda and Zimbabwe, both *in vivo* and *ex vivo* estimates of pathogenic fitness for the different HIV-1 group M isolates were determined. In Uganda, there are two dominating circulating subtypes – subtypes A and D. In Zimbabwe, subtype C is the dominant group M strain. Because of the subtype distribution in these different regions, generalizations about

subtype fitness can be made for these different countries. Firstly, women infected with subtype C were shown to have a slower rate of CD4+ T cell decline/week as opposed to subtype D, with the highest rate of decline⁹⁰. In reference to the country regions, these results translate to women from Zimbabwe having a slower rate of decline compared to those from Uganda. The 2-fold slower decline in Zimbabwean women in the absence of disease translates to 2-5 years of longer asymptomatic disease. After grouping the women into slow (stable CD4 counts above 350 and viral loads <2000 copies/ml in plasma for >3 years post-infection) and fast (CD4 decline to below 200 cells/ml within 2 years of infection) progressors, no woman infected with subtype D was classified as slow progressors in contrast to the 10% of women in this classification being infected with subtype C⁹⁰. The faster disease progression by HIV-1 subtype D was also confirmed by studies examining cohorts in Brazil⁹¹ and in a separate study in East and Southern Africa⁹². To take it further, Venner and his colleagues isolated the viruses from the cohort, PCR amplified the *env* gene, and cloned it into pREC_nfl_{NL4-3}Δenv. After producing these *env* chimeric viruses, competition experiments against one of two subtype B *env* chimeric viruses in PBMCs or primary CD4+ T cells were used to determine the relative replicative fitness. Subtype D viruses could compete with the subtype B viruses whereas subtype A viruses were less fit⁹⁰. However, subtype C viruses were completely outcompeted by the subtype B viruses and demonstrated low replicative fitness. Venner and his colleagues concluded based on their findings that subtype C is less virulent in humans when compared to subtypes A and D, with subtype D being the most virulent⁹⁰. They discuss the possibility of this playing a role in the disproportionate expansion and dominance of subtype C in the

global epidemic. With 2-5 more years of asymptomatic disease, HIV-1 subtype C may have more opportunities for infection.

1.7 Subtypes and Transmission Fitness Differences

There is currently limited and conflicting observational evidence that investigates transmission fitness differences between dominant HIV-1 group M subtypes. In a study done in Rakai, Uganda, Kiwanuka and his colleagues identified 260 HIV-1 positive discordant monogamous couples during a 5 year study period⁹³. Since Uganda has two dominating circulating subtypes, subtypes A and D, Kiwanuka and his colleagues could attempt to discern whether or not there were differences in transmission efficiencies between these two subtypes. For these couples, one partner was confirmed HIV-1+ and they followed the HIV-1- partner until seroconversion and retroactively identified the subtype between the couples. After adjusting for the appropriate variables, Kiwanuka and colleagues found that subtype A viruses were associated with a higher rate of transmission in comparison to subtype D viruses⁹³. Although this suggests transmission differences between subtypes may exist, it was limited in that other group M subtypes, such as subtype C, was not investigated. Thus, for Kahle and colleagues they conducted a nested-case control analysis using data from two prospective cohort studies of heterosexual HIV-1 discordant monogamous couples in Africa⁹⁴; in this study, subtypes A, C, and D's risk of transmission was investigated. In this analysis, subtype C was not associated with increased transmission risk in comparison to non-C subtypes⁹⁴. Moreover, when subtype C was compared to each of the subtypes individually, it was also not associated with an increased transmission risk. Lastly, even when they compared transmission risk between subtypes A and D, there were no significant differences. Altogether, the conflicting results of these two

studies indicate that further studies need to be done to fully discern the presence or absence of transmission fitness differences between the group M subtypes.

To date, only preliminary studies using the same pairwise competitions described earlier have attempted to estimate the transmission fitness of the different dominant group M subtypes. Initial studies showed subtype C to have relatively equal ability to replicate in skin-derived Langerhans cell cultures compared to subtype B⁸⁵. In an *ex vivo* assay that utilized explanted genital tissue, HIV-1 subtype C could compete with, and sometimes even win, against subtypes A and D isolates when examining replication in the tissue⁸¹. However, when *trans*-infection experiments were performed downstream, subtype C was outcompeted by the other subtypes. It is also important to note that consistent with previous findings, this same study found that only R5 isolates could replicate in the tissue, whereas X4 viruses could not⁵⁵.

Altogether, these limited studies may suggest that subtype C has comparable transmission efficiencies to other dominant group M subtypes even with a lower replicative ability. Here, we tested whether acute HIV-1 subtype C viruses transmitted more efficiently in comparison to acute subtypes A, B, and D using the *ex vivo* human explant assay. In this study, eight *env* chimeric viruses that contain the pREC_nfl_{NL4-3}Δenv backbone and the *envelope* region from acute primary isolates were used. Using various mixtures of the different subtype viruses, competition experiments were performed on both foreskin and cervical explant tissue. In addition, competitions were performed on a T cell clone permissive to HIV-1 infection (PM1) to assess the different subtypes' replicative ability.

1.8 Hypothesis and Aims

As discussed, what defines a virus' ability to replicate in susceptible cells and cause pathogenesis may be different than what defines its ability to transmit efficiently across the genital mucosa. Although evidence shows that HIV-1 subtype C has the lowest replicative fitness and causes the slowest disease progression, I hypothesize that HIV-1 subtype C will have the highest transmission fitness and transmit the most efficiently in our *ex vivo* explant model. To explore this hypothesis, we sought to 1) propagate and titre large volumes of HIV-1 chimeras that contain the *envelope* from subtypes A-D acute primary viruses; 2) compete these viruses in round robin on cervical and foreskin explant tissue; 3) assess the ability of the different subtypes to replicate in the tissue and be transported out of the tissue by migrating cells for replication in susceptible T cells; and 4) compare the transmission fitness of the subtypes to their abilities to replicate directly on PM1 cells. The work presented here will help provide insight into whether or not there are differences in transmission efficiencies between the dominant HIV-1 group M subtypes and the relationship to their abilities to cause pathogenesis.

Chapter 2: Materials and Methods

2.1 Cells

U87.CD4.CCR5 cells were obtained from the NIH AIDS Reagent Program. U87.CD4.CCR5 cells were the cell types used to propagate large amounts of virus. These cells are human glioblastoma cells that express both receptors required for sexual transmission of HIV-1. These cells were chosen for propagation because they are easily infectable and exhibit syncytia when infected. U87.CD4.CCR5 cells were cultured in 10% FBS-DMEM supplemented in 1% penicillin/streptomycin, 300 µg/mL G418, and 1 µg/mL puromycin (DMEM complete). G418 selects for cells expressing CD4 and puromycin selects for cells expressing CCR5.

For *trans*-infection studies in the explant model and replicative fitness experiments, PM1 cells were used. PM1 cells are a clonal derivative of HUT 78, a cutaneous T lymphocyte. These cells are permissive for growth of macrophage and T cell tropic viruses, such as HIV-1. PM1 cells were obtained from the NIH AIDS Reagent Program and cultured with 10% FBS-RPMI supplemented with 1% penicillin/streptomycin (RPMI complete).

2.2 Virus Cloning and Propagation

A complete list of viruses used in this study can be found in **Table 1**. Acute primary subtype B viruses were obtained from the Center for HIV/AIDS Vaccine Immunology (CHAVI) acute infection studies. The study initiated in June 2006 and ended in June 2013. During this time, group 1 participants characterized by people with acute HIV infection began enrolling and blood collection occurred. Primary subtype A, C, and D viruses were obtained from women enrolled in the Hormonal Contraception and Risk of HIV

Acquisition Study in Uganda and Zimbabwe⁹⁵. Upon primary HIV-1 infection, women were enrolled into a subsequent study, the Hormonal Contraception and HIV-1 Genital Shedding and Disease Progression among Women with Primary HIV Infection (GS) Study⁹⁶⁻⁹⁸ (**Table 1**). Blood and cervical samples were collected every month for the first six months, then every three months for the first two years, and then every six months up to 9.5 years. DNA was extracted from patient's PBMC samples obtained at the seroconversion visit and every three months post HIV infection. The entire gp120 coding region and extracellular domain of gp41 (referred to as *env* DNA) was PCR amplified from PBMC DNA derived from the seroconversion visit for subtypes A, C, and D. The same amplification procedure was done for subtype B viruses obtained from group 1 of the CHAVI acute infection studies. This was done to ensure as close of a representation to the transmitted/founder (T/F) virus.

All HIV-1 *env* genes from acute infection samples were cloned and propagated using a protocol previously described⁹⁹ (**Figure 3**). HIV-1 *env* was the region of interest due to studies showing its role in sexual transmission of HIV-1 and defining characteristics of the T/F virus⁷²⁻⁷⁴. The HIV-1 *env* gene was cloned into pREC_nfl_{NL4-3}Δenv/URA3 using yeast recombination/gap repair. Positive colonies signified successful recombination as colonies did not survive with the uracil gene still present in the vector. The pREC_nfl construct containing the HIV-1 *env* from acute infection samples was co-transfected into 293T cells together with a complimenting vector pCMV_cp1t to produce fully infectious particles. My work relevant to this research project started here, where I expanded virus quantities for downstream assays. To do this, I infected U87.CD4.CCR5 and harvested virus after 3, 7, 10, and 14 days of culture.

Table 1. Acute env chimeric viruses used in this study

VIRUS ID	PARTICIPANT DESIGNATION	INFECTION GROUP	SEX	TRANSMISSION	PHENOTYPE	SUBTYPE
63UR	GS-0221-03	Acute	F	Heterosexual	R5	A
15U	GS-0054-07	Acute	F	Heterosexual	R5	A
13U	GS-0043-07	Acute	F	Heterosexual	R5	A
B4	WEAUd15.410. 787	Acute	M	MSM	X4/R5	B
B7	SC05.8C11.234 4	Acute	M	Heterosexual	R5	B
23Z	GS2003	Acute	F	Heterosexual	R5	C
6Z	GS2182	Acute	F	Heterosexual	R5	C
14U	GS-0048-07	Acute	F	Heterosexual	R5	D

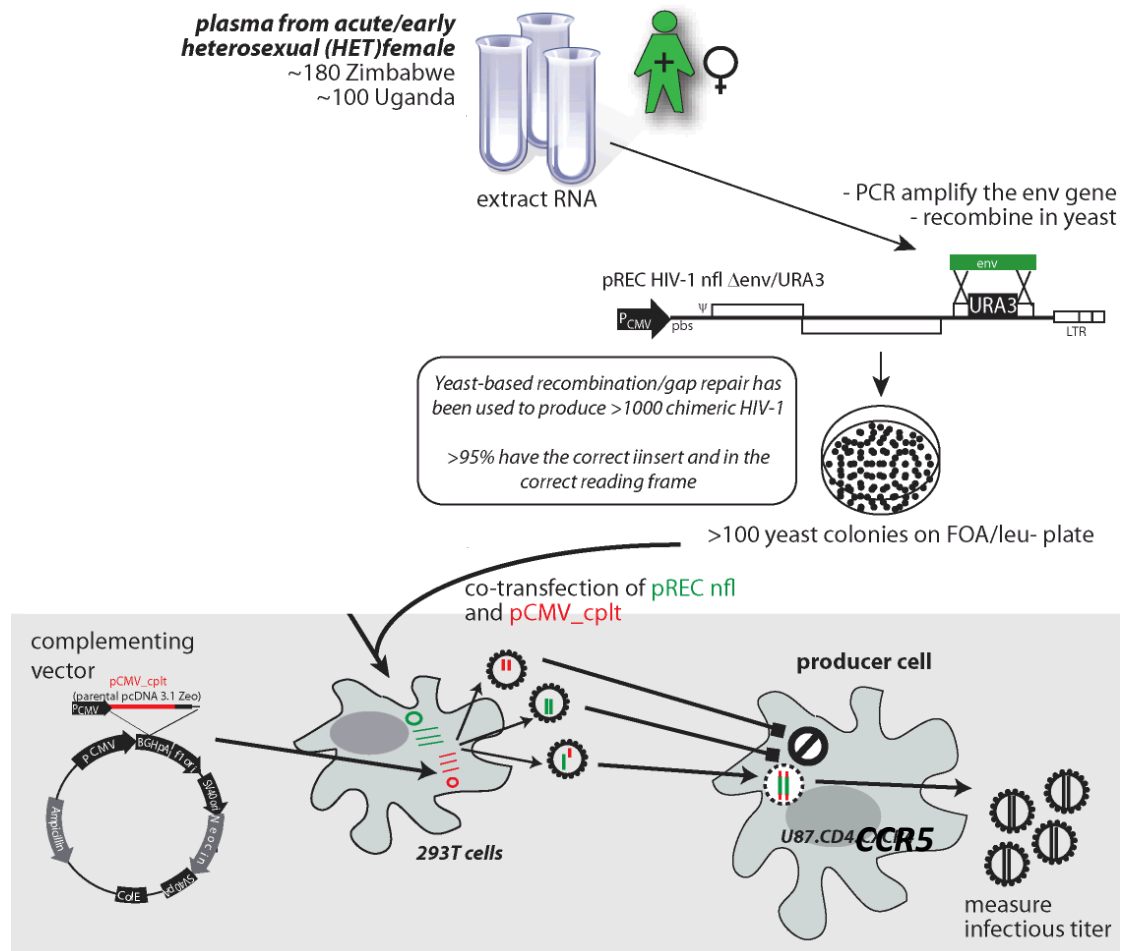


Figure 3. Schematic of PCR amplification of HIV-1 env and cloning into pREC_nfl_{NL4-3} Δ env/URA3 (courtesy of Dr. Eric Arts)

The entire gp120 coding region and extracellular domain of gp41 (termed *env* DNA) was PCR amplified from DNA derived from PBMCs isolated during the seroconversion visit and acute infection. This *env* product was cloned into pREC_nfl_{NL4-3} Δ env/URA3 via yeast recombination/gap repair. After isolating the new pREC_nfl vector containing *env* from patient DNA, it was co-transfected with a complementing vector in 293T cells to produce fully infectious viral particles. Subsequent viral propagation was performed in U87.CD4.CCR5 cells.

2.3 Virus Quantification

Median tissue culture infectious dose (TCID₅₀) was determined for each virus in **Table 1**. TCID₅₀ values are a measure of infectious titre and quantifies the amount of virus required to kill or produce a cytopathic effect in 50% of inoculated tissue culture cells. Quantifying the titres of the propagated viral stocks were needed for infection in the explant assay. Ten thousand U87.CD4.R5 cells were seeded on a 96 well plate for virus infection (4 viruses/plate). The following day, cells were infected, in triplicate, with virus stocks from day 7 harvests that were serially diluted from neat to 1:10⁷ (**Figure 4**). Reverse transcriptase (RT) activity of the supernatant of infected cells were used to calculate TCID₅₀ values of the viruses using the Reed-Muench Method^{100,101}. This method calculates the number of infected cells observed to TCID₅₀ values.

RT activity was determined using the well-established radioactive RT assay on the supernatant of infected U87.CD4.R5 cells^{102,103}. Briefly, 10uL of supernatant from the infected cells was mixed with 20uL of RT master mix [50mM Tris-HCl (pH 7.8), 75mM KCl, 2mM dithiothreitol, 5 mM MgCl₂, 5ug of poly(rA)-poly(dT) per ml, 0.5% (vol/vol) NP-40, 1uL of fresh 10-mCi/ml[α-³²P]TTP per ml]. The RT master mix lysed the virus but maintained functionality of the RT and supplied radioactive nucleotides. Thus, any functional RT from the virus will make new DNA with radioactive nucleotides incorporated. This radioactivity can then be imaged on a screen.

After incubation for 2 hrs at 37°C, the samples were blotted onto a diethylaminoethyl cellulose (DEAE-C) filter mat. The positively charged diethylaminoethyl groups can bind

the negatively charged DNA. The filters were allowed to dry, washed with a saline-sodium citrate (SSC) buffer (0.15M NaCl, 0.015M sodium citrate) five times, rinsed two times with 80% ethanol, and dried once more. The filters were then placed in a phosphor screen overnight to expose the screen to the radiation from RT-produced DNA. The next day, it was imaged with Storm 820 Phosphorimager to scan the phosphor screens for positive signals. These positive signals represent RT activity and were used to calculate TCID₅₀ values.

2.4 RNA Extraction and RT-PCR for DNA Sequencing and Subtyping

In order to confirm the subtype of the different viruses used, RNA from the propagated viral stocks were extracted for subsequent RT-PCR. RNA extraction was performed using the QIAGEN RNeasy Mini kit as per manufacturer's instructions and eluted in RNA-free, DNA-free H₂O (sigma H₂O). QIAGEN's One-Step RT-PCR Enzyme mix and primers specific to the gp120 region (ENVB, ED14) were used to perform first round RT-PCR (**Table 2**). Ampure XP Beads were used to purify the cDNA product with subsequent second round PCR amplification using 2X KAPA HiFi HotStart Ready Mix and primers specific to the C2-V3 *env* region (E80, E125). PCR cycle conditions for the 1st round were 50°C for 30min, 95°C for 15 min, followed by 35 cycles of 94°C for 30s, 55°C for 30s and 72°C for 90s, and a final extension of 72°C for 10min. The PCR conditions for the 2nd round were 95°C for 3 min, followed by 25 cycles of 95°C for 30s, 55°C for 30s and 72°C for 30s, and a final extension of 72°C for 10min. Each C2-V3 *env* sequence was phylogenetically aligned with a set of reference subtype A, B, C, and D viruses obtained from Los Alamos National Laboratory's HIV sequence database¹⁴, trees were constructed via Muscle and maximum likelihood methods in MEGA X¹⁰⁴.

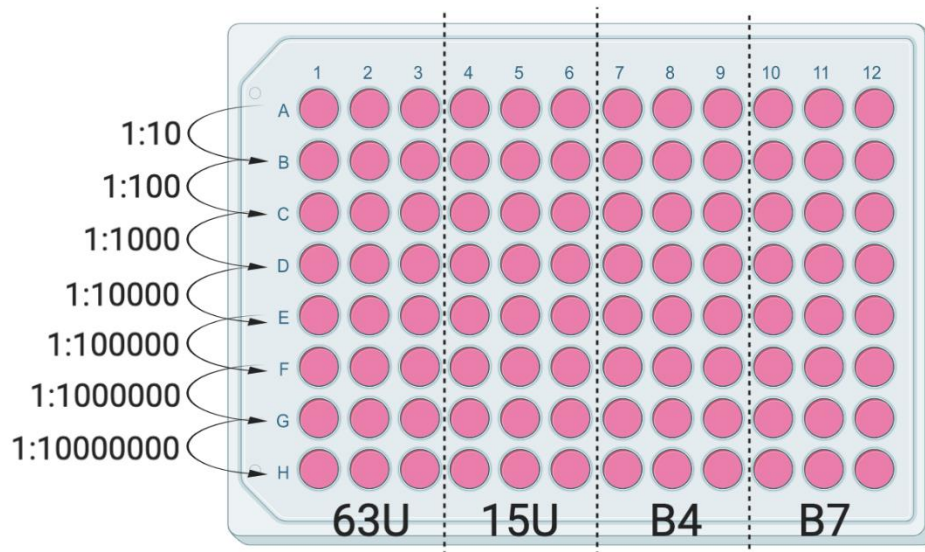


Figure 4. Example of RT Assay protocol, quantifying four viruses

Ten thousand U87.CD4.CCR5 cells were seeded on 96 well plate on day 0. On day 1, viral stocks were titrated and cells were infected in triplicate, as shown. Reverse transcriptase activity measured in the supernatant was used to calculate TCID₅₀ values of the viruses using the Reed-Muench Method.

Table 2. DNA Primers used in this study

PRIMERS	PRIMER SEQUENCE (5' → 3')
ENVB	AGAAAGAGCAGAAGACAGTGGCAATGA
ED14	TCTTGCCTGGAGCTGTTTGATGCCCCAGAC
E80 W/ ILLUMINA TAG	<i>TCGTCGGCAGCGTCAGATGTGTATAAGAGACAGCCAATTCCCATACATT</i> ATTGTG
E125 W/ ILLUMINA TAG	<i>GTCTCGTGGGCTCGGAGATGTGTATAAGAGACAGCAATTTCTGGGTCCC</i> CTCCTGAGG
GAG-CONS1	GAGAGAGATGGGTGCGAGAGCG (HXB2 783-804)
UNIV-GA4	TTGCCAAAGAGTGACCTGAGGGAA (HXB2 2250-2273)
GSCA F	CATGTTTTCAGCATTATCAGAAGGA (HXB2 1299-1323)
GSCA R	TGCTTGATGTCCCCCACT (HXB2 1359-1377)
GSCA PROBE	6-Fam-TACTGGGACAGCTACAACCATCCCTT-BHQ (HXB2 968-993)

***Illumina Tag**

2.5 *Ex vivo* Tissue Explant Assay

Explanted genital tissue was used to assess the relative transmission fitness of the viruses listed in **Table 1**. Cervical tissue was obtained from the National Disease Research Interchange (NDRI) tissue bank in Philadelphia, USA¹⁰⁵. NDRI collects tissues from over two hundred sites under rigorous reviews and strict government regulations; ethical approval, consent forms, and patient data are kept at their site. Anonymously donated foreskin tissue was obtained from adult men (>18) undergoing elective circumcision (for cosmetic or cultural reasons) at the University Urology Associates (UUA) clinic in Toronto.

Viruses in **Table 1** were combined and used to infect genital explant tissue in “competitions” to assess relative transmission fitness (**Figure 5**). Each of the eight competitions consisted of 4 different viruses, where each virus was eventually competed with all others through a round-robin design (**Table 3**). In this assay, when a given virus gets the opportunity to establish infection it will take over and outcompete all the other viruses. Consequently, if all eight viruses were competed against each other at once, the ability to elucidate a relative transmission fitness order would not be possible and thus, a round-robin design is used. Additionally, four competitions from **Table 3** (5-8) excluded subtype D. Due to the dominance of subtype D in my results, it was removed to attempt to discern the relative transmission fitness differences of the other subtypes.

Genital tissue was cut into ~3 mm³ blocks, placing three pieces of tissue per well in a 48-well flat-bottom plate. Tissue was suspended in 10%FBS-RPMI complete media and exposed to a mixture of viruses at either a multiplicity of infection (MOI) of 0.01 each (150 infectious units, IU) or 5x this (MOI 0.05; 750IU) for 6 hours (**Table 3**). Each competition

was performed in duplicate for each donor. After this, the inoculating mixture was discarded and tissue was washed twice with 250uL of PBS to remove any input virus. Subsequently, tissue was cultured in 10%FBS-RPMI complete media for 24 hours in the same well.

Tissue pieces were then removed with sterile forceps, washed once with 250uL of PBS, and placed in one well of a 96-well U-bottom plate and cultured in 10%FBS-RPMI complete media supplemented with Normocin (anti-fungal) for 10 days. After removal of the tissue, migratory cells (MC) emigrating from the tissue were harvested. To do this, culture media was removed from the wells and placed into a 1.5mL Eppendorf tube. After tubes were spun at 1500g for 5min, the liquid was decanted and 250uL of PBS was added to the tube. This spin-wash step was repeated once more with a final decanting step. A small pellet was observed frequently. Forty thousand PM1 cells were then seeded per well in a 96-well U-bottom plate. The pellet in the Eppendorf tube was resuspended and co-cultured with the PM1 cells in 10%FBS-RPMI complete media for 10 days. For tissue culture and migratory cell/PM1 co-cultures, media was changed every 3 days.

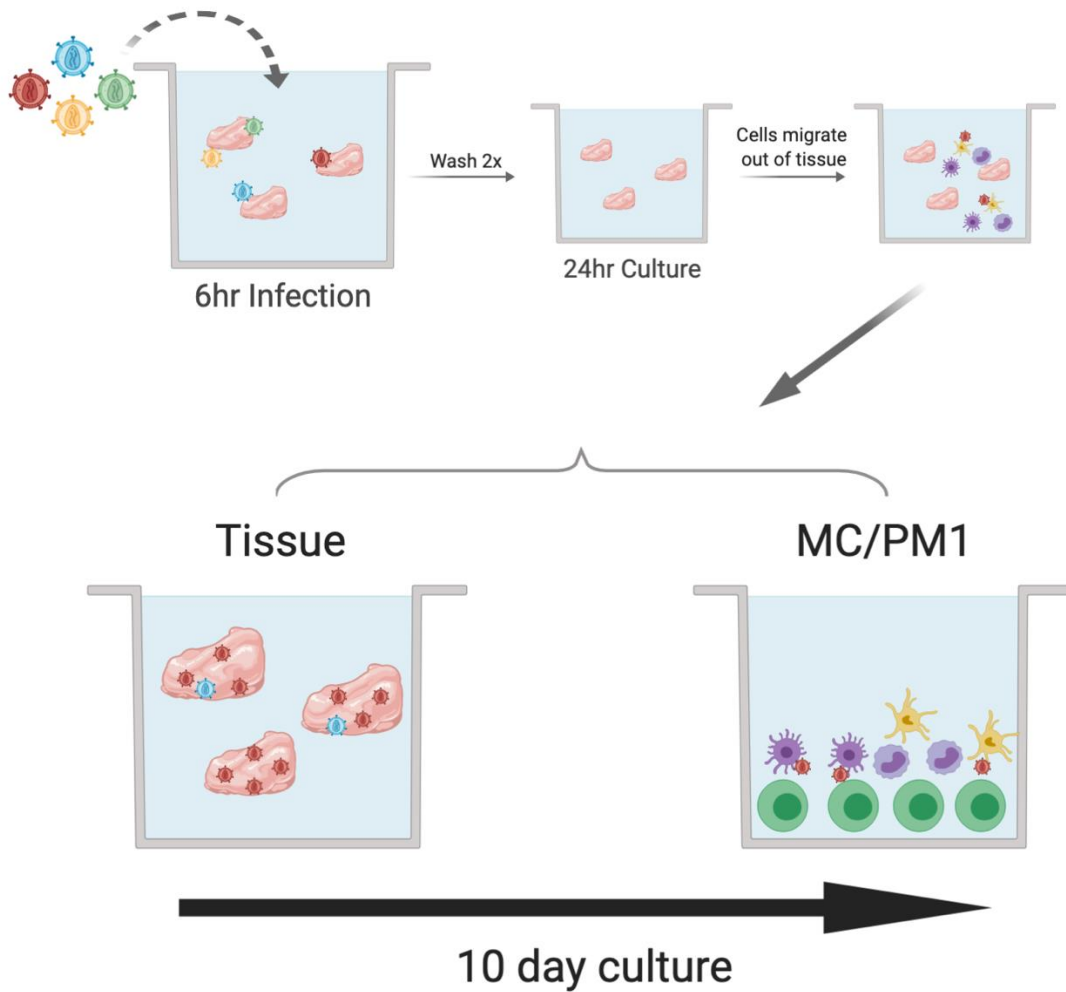


Figure 5. Experimental protocol for the ex vivo explant assay

Three $\sim 3 \text{ mm}^3$ pieces of cervical or foreskin tissue were infected with a mixture of viruses in Table 3 for 6 hours. After washing the tissue thoroughly to ensure input viruses were removed, tissue was cultured for 24 hours. Following this 24 hour culture, migratory cells were collected from the supernatant and co-cultured with a clonal T cell line, PM1, for 10 days. Concurrently, tissue was cultured for the same amount of time.

Table 3. Acute env chimeric viruses included in each competition

COMPETITION	VIRUSES
1/A	15U x B4 x 6Z x 14U
2/B	15U x B7 x 23Z x 14U
3/C	63U x B4 x 6Z x 14U
4/D	63U x B7 x 23Z x 14U
5/E	15U x B4 x 23Z x 13U
6/F	15U x B7 x 6Z x 13U
7/G	63U x B4 x 23Z x 13U
8/H	63U x B7 x 6Z x 13U

2.6 Direct Competitions on PM1 cells

To assess the relative replicative fitness of the different subtypes, the same competitions in **Table 3** were directly exposed on PM1 cells. Forty thousand PM1 cells were seeded per well in a 96-well U-bottom plate in 10%FBS-RPMI complete media. PM1 cells were subsequently infected with 200 IU of each virus (MOI 0.005) for 3 hours and after this time the supernatant was removed and 250uL of new media was added. This was cultured concurrently with the explant assay for 10 days and media was changed every 3 days during this time.

2.7 DNA Extraction and PCR Amplification

After the 10 day culture of both tissue and MC/PM1s, the explant assay was completed. At completion of the assay, tissue, MC/PM1 co-cultures, and PM1 cells were lysed and DNA extracted with either the QIAGEN DNeasy Blood and Tissue, or the 96-well format of the kit, QIAGEN DNeasy 96 Blood and Tissue Kit, both as per manufacturer's instructions. Briefly, tissue was lysed overnight with the provided Proteinase K solution at 56°C; MC/PM1 co-cultures and PM1 cells were lysed with the Proteinase K solution for 10 min at 56°C. After lysis, the lysate was passed through the DNeasy Mini Spin Column or plate. The DNA was then spin-washed with the provided buffers in two steps and then eluted in sigma H₂O.

Two rounds of PCR amplification were performed with primers specific to the C2-V3 *env* region (**Table 2**). A set of external primers, ENVB and ED14, were used for the first round of amplification (gp120-coding region of *env*, ~1.7kb). This was followed by a set of nested primers, E80 and E125 w/ Illumina tag, which was used for the second round of

amplification (C2-V3 *env* region, 0.48 kb) (**Figure 6**). PCRs contained 0.2 μ M of each primer, 1.5 mM MgCl₂, 5x Platinum Taq PCR buffer, 0.2 mM dNTPs and 2 units Platinum Taq DNA polymerase. The amount of template for the external and nested PCR was 20uL and 5uL, respectively. PCR cycle conditions were 95°C for 2min, followed by 35 cycles of 95°C for 30s, 55°C for 30s and 72°C for 2min (external) or 45s (nested), and a final extension of 72°C for 10min. Successfully amplified PCR products were confirmed on a 1% agarose gel to verify product size of 480 bp. Samples that did not PCR amplify were repeated twice.

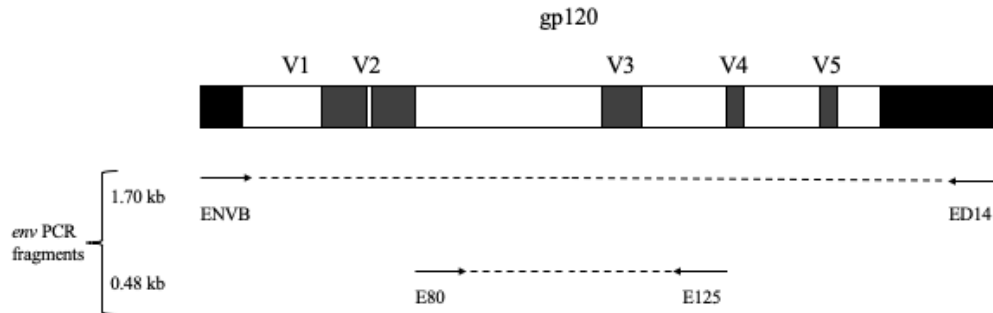


Figure 6. PCR strategy for Next-Generation Sequencing

The C2-V3 *env* region was PCR amplified in two rounds for subsequent NGS analyses.

The first round produced a 1.70 kb product with the final product being the C2-V3 *env* region - 0.48 kb of gp120.

2.8 Next-Generation Sequencing Library Preparation and Sequencing

To perform next-generation sequencing on the PCR amplicons, the sequences need to be tagged with a barcode and combined and pooled in equivalent amounts (**Figure 7**). Purification of the successfully amplified PCR amplicons and normalization of their concentrations was performed using SequalPrepTM Normalization Plate Kit, as per the manufacturer's instructions. This plate utilizes ChargeSwitch Technology that allowed a switchable surface charge depending on the pH of the surrounding buffer. This allowed for purification, binding of ~25ng of DNA, and elution at a certain concentration. In a three step process, PCR amplicons were bound to the plate after a 1 hour incubation, subsequently washed, and then eluted in water to achieve an expected DNA concentration of 1-2 ng/ul.

Illumina's Nextera XT DNA Library Preparation Kit was used to prepare up to 384 purified and normalized PCR amplicons at one time. Using a one-step process called tagmentation, the DNA is simultaneously fragmented and tagged with an adaptor sequence. A limited PCR cycle then used the adapters as primers to amplify the tagged DNA while adding index adaptor sequences to both ends; this allowed for pooling of the library (**Figure 7**). After this, normalization and purification with SequalPrep was performed once more.

Sequencing was performed by Illumina's MiSeq System at the London Regional Genomics Centre at the Robarts Research Institute at Western University. The samples were sequenced using the MiSeq 600 cycle Reagent Kit v3, which extends read lengths up to 2 x 300 bp. The sequences were then analyzed by Illumina's Metagenomics app, BaseSpace.

Simply, this app automatically converts the sequence data to FASTQ format and provides the user with a multitude of genomic analysis apps.

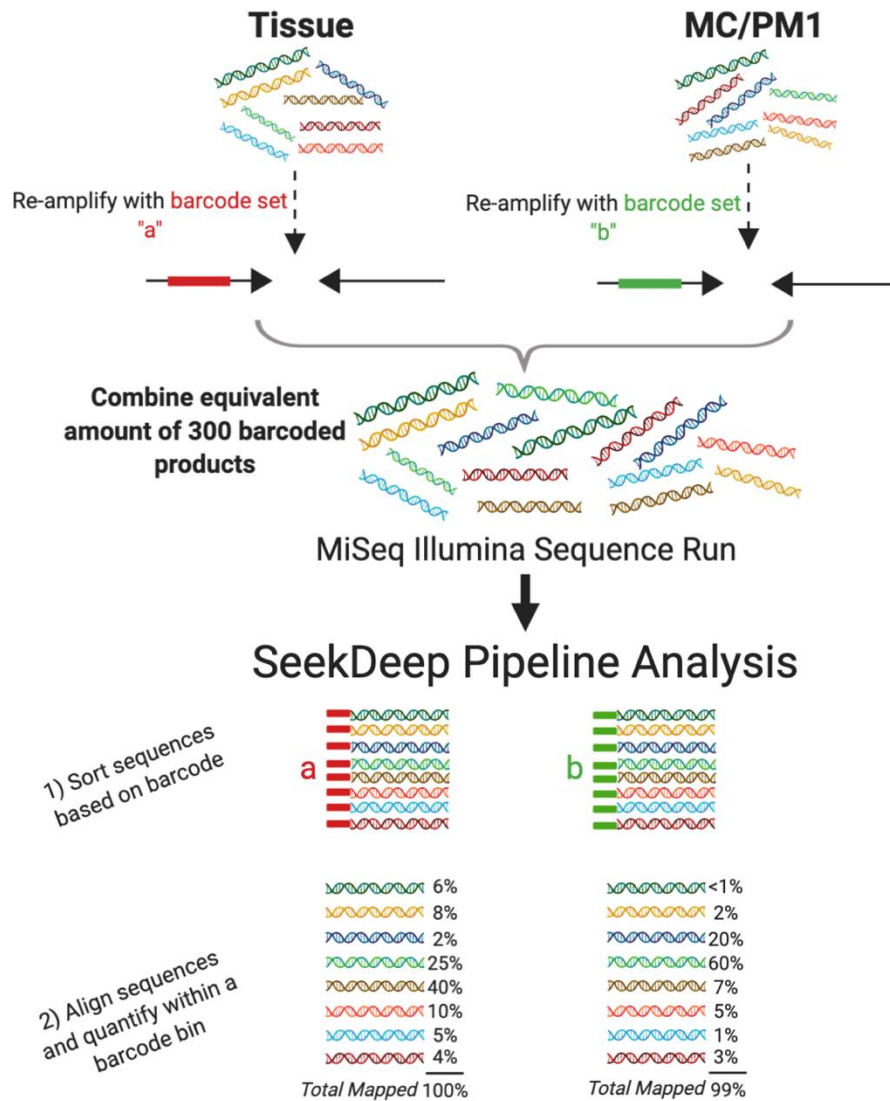


Figure 7. NGS preparation and sequence analysis pipeline

After PCR amplification, sequences were re-amplified with different barcode sets according to their respective assay compartments (tissue vs. MC/PM1). After this, all sequences were pooled and sequenced using MiSeq. SeekDeep (Hathaway et al, 2012), a pipeline to determine haplotype frequencies was employed on the sequences.

2.9 Sequence and Statistical Analysis

Sequence data was analyzed by Dr. Jeff Bailey's group at Brown University using their SeekDeep pipeline¹⁰⁶. This open source pipeline allows for haplotype frequency estimation on targeted sequencing data for multiple samples in a population. In this case, the haplotype in question is the C2-V3 *env* region of a given virus. Briefly, their pipeline demultiplexes on the samples, clusters and collapses unique reads, and undergoes final filtering and alignment of the population to sequences of the known input viruses to give a relative abundance of each virus sequence in each competition as a proportion of 100 (**Figure 7**).

Subtype comparisons were performed by averaging relative abundance from the technical replicates of each virus and then taking the average of those averages for all the viruses in a single subtype. For example, in competition 1 (**Table 3**) the relative abundance of virus 15U was averaged across its technical replicates. After this was done for every single virus in every competition, the relative abundance of 63U, 13U, and 15U, all the subtype A viruses employed in this study, were averaged across all a) competitions that included all subtypes (1-4); and b) competitions that excluded subtype D (5-8). This allowed the comparison of the average relative abundance of subtype A, in comparison to the other subtypes, across all a) competitions that included all subtypes; and b) competitions that excluded subtype D. Means values with SEM are presented.

2.10 Quantitative Polymerase Chain Reaction (qPCR)

In a 50uL reaction, an external PCR was initially completed using primers gag-cons1 and UNIV-GA4 (**Table 2**). Following this PCR, 5uL of the PCR product was added to the TaqMan Fast Advanced Master Mix in addition to primers gsca F, gsca R, gsca probe.

Samples were run using the QuantStudio5 Real-time PCR system under the following reaction conditions: 60°C for 2min, 95°C for 20s, 40 cycles of 95°C for 1s and 60°C for 43s. All samples were run in duplicate. Samples were considered negative when CT values were above 35.

Chapter 3: Results

3.1 Virus Quantification and Titres

Acute *env* chimeric viruses were previously generated by past members of the Arts Lab⁹⁰. To ensure equal opportunity for infection in the explant assay for all viruses utilized, viral stocks were titred on U87.CD4.CCR5 cells using the standard TCID₅₀ method after large-scale propagation. Phosphor images displayed the number of positive signals per row of triplicate as dilutions increased 10-fold per row going down (**Figure 8**). The first row of each virus frequently did not have any positive signal, most likely due to cytopathic effects of infection. Using the Reed-Muench Method, viral titres were quantified (**Table 4**). Virus 63U had the highest titre of 2.18×10^6 IU/mL and 14U had the lowest titre of 1.03×10^3 IU/mL. Due to 14U's low titre, larger volumes of this virus were utilized for the competition experiments. As such, propagation of 14U was done more than once which meant an additional RT assay needed to be performed.

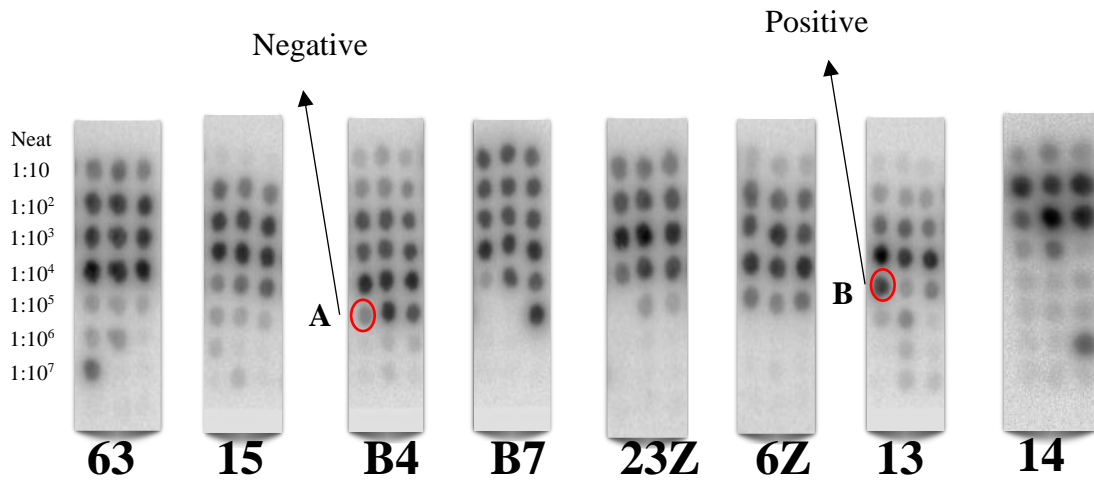


Figure 8. Phosphor Images produced from RT assay of each virus used in the study

Each row of three corresponds to one dilution factor with the top row being the most concentrated and the last row being the least concentrated. The top row frequently showed no positive signals due to high concentration of virus. Day seven harvests of each virus were used. **(A)** Lighter signals did not count as positive when compared to intensity of signals in the upper rows. **(B)** An example of one positive signal in a row with two negative signals.

Table 4. Viral titres calculated using the Reed-Muench Method, corresponding to positive signals in phosphor images

VIRUS	TITRE (IU/ML)
63U	2,181,971.59
15U	122,701.279
B4	1,227,012.79
B7	218,197.159
23Z	122,701.278
6Z	218,197.159
13U	218,197.159
14U*	1035.904; 1851.06

**two different propagations*

3.2 Subtype Confirmation

To confirm that the viral stocks used for propagation belonged to the expected subtype, RT-PCR was performed on propagated virus with subsequent phylogenetic analysis. Using reference sequences from Los Alamos National Laboratory's HIV sequence database, the C2-V3 *env* region of the different subtype chimeric viruses were aligned with those from the sequence database. As expected, phylogenetic analysis demonstrated the presence of three HIV subtype A (63U, 15U, 13U), two subtype B (B4, B7), two subtype C (23Z, 6Z), and one subtype D (14U) virus (**Figure 9**).

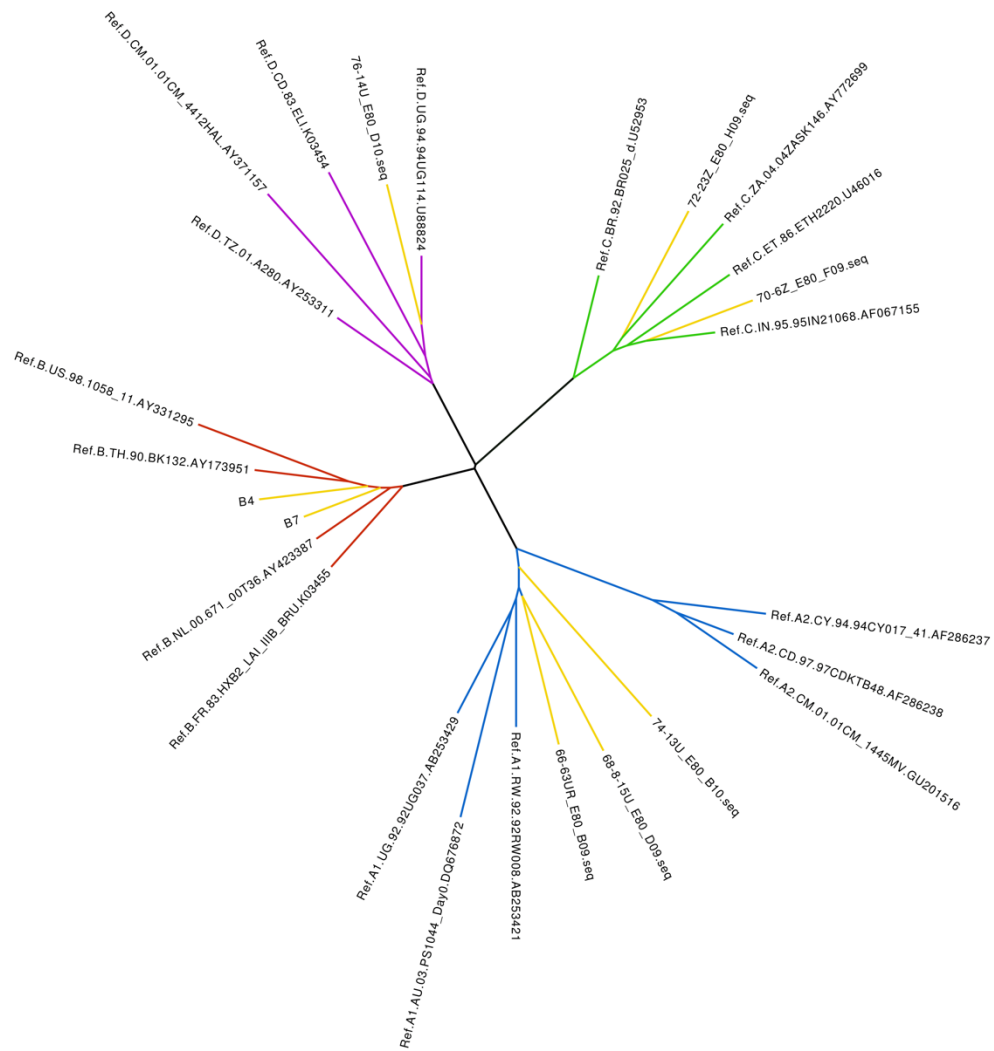


Figure 9. Phylogenetic alignment for subtype identification of each env chimeric virus

Reference HIV-1 sequences were obtained from Los Alamos National Laboratory’s HIV sequence database and aligned with the C2-V3 *env* region from the viruses used in this study. Maximum likelihood tree was generated via MEGA X. Open shapes represent the reference sequences and filled-in shapes represent the viruses used in this study. Blue = Subtype A, Yellow = Subtype B, Red = Subtype C, and Green = Subtype D.

3.3 Direct Competitions on PM1 cells to Assess Replicative Fitness

To understand whether transmission fitness may be different than replicative fitness, the competitions in **Table 3** were performed directly on PM1 cells. As discussed, the replicative or *pathogenic* fitness of a virus strain can be defined as the relative *ex vivo* replication capacity of HIV-1 in CD4+ T cells and/or PBMCs^{82,83}. Thus, forty thousand PM1 cells were infected with 200 IU of each virus (MOI 0.005) for 3 hours and cultured concurrently with the explant assay for 10 days.

Figure 10 provides a summary figure that mirrors the same analysis done for transmission fitness. Subtype D was the most effective at replicating in PM1 cells, at around 80%, with subtype B consisting of almost 20% of viral replication. Subtypes A and C were outcompeted by subtypes B and D, with very low levels of replication measured in PM1 cells. When subtype D was removed from the competition, there was no observed differences in the replication of the different subtypes.

Figure 11 provides the same data as **Figure 10**, but showing the results of each individual competition with viruses grouped by subtype (competitions performed in duplicate, average of replicates shown). Panels E-H, the four competitions that excluded subtype D, showed inconsistent results with which subtype replicated more effectively. Competitions 5 and 8 (Panels E and H) showed subtype C to be the most effective, while competitions 6 and 7 (panels F and G) had subtype A as the “winner”. Subtype B never outcompeted both subtypes, outcompeting only subtype A in panels E and H and only subtype C in panel F. As such, drawing conclusions from summary **figure 10B** is challenging.

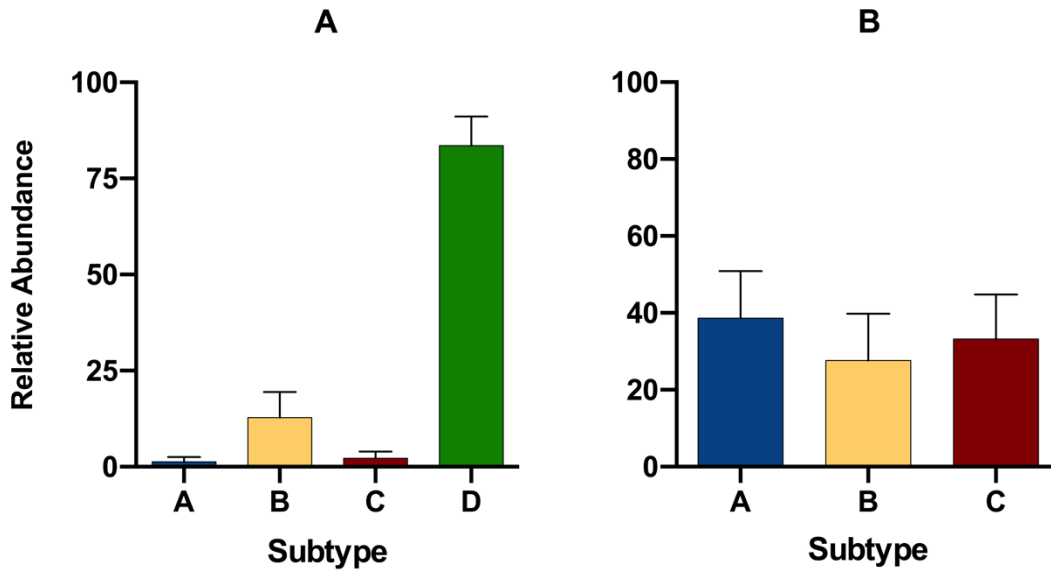


Figure 10. Average relative abundance of each subtype in PM1 cells

40,000 PM1 cells were infected with 200 IU of each virus for a MOI of 0.005. After 3 hour infection, cells were cultured concurrently with the explant assay for 10 days. Competitions were performed in duplicate. The average relative abundance of each across all eight competitions are presented. **(A)** Competitions including all four subtypes; **(B)** competitions excluding subtype D. Mean values with SEM are shown.

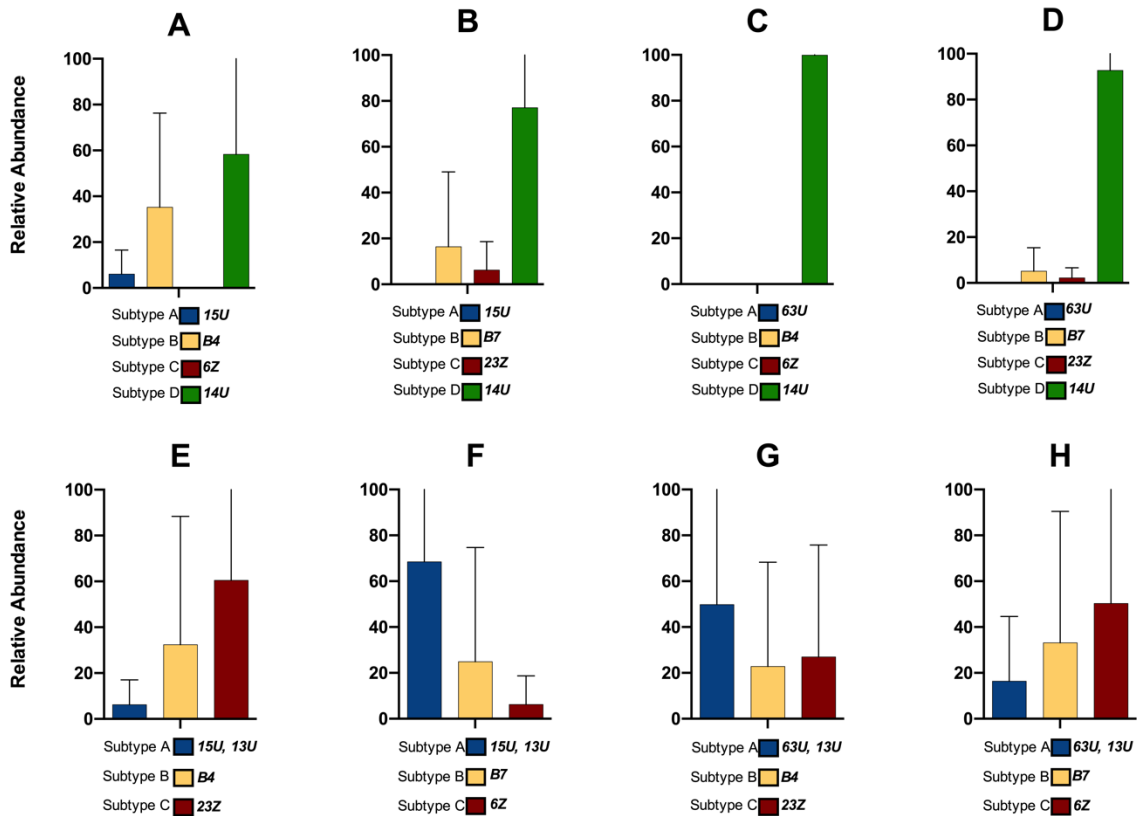


Figure 11. Individual multi-virus competitions performed on PM1 cells, grouped by subtypes

(A-H) 40,000 PM1 cells were infected with different mixtures of *env* chimeric viruses as shown below the graphs. Competitions were performed in duplicate. The average relative abundance of each subtype in each specific competition in PM1 cells are presented. Mean values with SEM are shown.

3.4 Multi-virus Competitions in Human Explant Tissue to Assess Relative Transmission Fitness

Three tissue pieces (each $\sim 3\text{mm}^3$) from cervical tissue were exposed to different mixtures of four acute *env* chimeric viruses. To simulate *trans*-infection events, after 24 hours the migratory cells were isolated and co-cultured with PM1 cells. At the end of the 10 day culture period, both compartments were lysed, proviral DNA was extracted, and sequences were PCR amplified and sequenced for alignment and counting via SeekDeep¹⁰⁶. It is important to note that although the tissue is washed well after initial viral inoculation, HIV-1 proviral DNA instead of HIV-1 RNA is extracted to further ensure the measuring of infection instead of residual inoculating virus.

Each of the eight competitions consisted of 4 different viruses, where each virus was eventually competed with all others through a round-robin design. Many studies from our group have observed a phenomenon where one virus in a mixture will take over and outcompete all the other viruses, in this assay. Consequently, if all eight viruses were competed together at once, the ability to elucidate a relative transmission fitness order would not be possible and thus a round-robin design is used. Four competitions (1-4, **Table 3**) included one of each subtype A, B, C, and D, while the four remaining competitions (5-8, **Table 3**) did not include a subtype D virus. Once again, competitions excluding subtype D were performed in light of the fact that it outcompeted all the other viruses. The combinations of viruses ensured that each virus was competed against all the other viruses in two different mixtures. For example, competition 4 has a mixture of 63U, B7, 23Z, and 14U and competition 8 also competes 63U and B7 against one another but in the presence of 13U and 6Z.

3.4.1 Using a low MOI may result in stochastic infection events that do not reflect differences in transmission fitness between subtypes

A multiplicity of infection (MOI) of 0.01 was initially used based on previous published studies in our group¹⁰⁷. Briefly, in an explant of $\sim 3\text{mm}^3$ there are approximately 5000 migratory cells¹⁰⁷. Thus, in an infection of three explant pieces there are $\sim 15,000$ migratory cells. With 150 IU of each virus added to the inoculating mixture, results using an MOI of 0.01 are summarized in **Figures 12 and 13**. The summaries compared the average relative abundance of each subtype, which is assumed to represent the average relative replication of each subtype, in both tissue and MC/PM1 co-cultures. **Figure 12** provides the average relative abundance across all eight competitions, separating the competitions that included subtype D virus 14U (Panel A) and those that did not (Panel B). **Figure 13** provides the same data as **Figure 12**, but showing the results of each individual competition, stratified by tissue donors (viruses of same subtype grouped).

Overall, the PCR efficiency from these competitions were very low (**Figure 14A**); an overall PCR efficiency of $\sim 45\text{-}50\%$ was measured. PCR efficiency was measured by the number of samples with amplified PCR products over the total number of samples. This was done to illustrate what I speculate as stochastic infection events. The PCR inefficiency of these competitions are also demonstrated in **Figure 13**, where some competitions did not have any measurable HIV-1 replication in the tissue and/or replication in MC/PM1 co-cultures (Panels B and E-H). Moreover, there was inconsistency when comparing the “winner” of the competitions between donors and between competitions. For example, in competition 4 (Panel D) there was higher replication of subtype B in donor A vs. subtype

A in donor B in MC/PM1 co-cultures. Additionally, in competitions 1 and 4 (Panels A & D) subtype C and D had equal levels of replication in donor A MC/PM1 co-cultures vs. subtype B being the “winner” in donor A MC/PM1 co-cultures. Overall, there was concern that any of the trends exhibited in **Figure 12** were due to stochastic events based upon the low PCR efficiency (**Figure 14**) and the inconsistency of results in **Figure 13**. To address the possibility of stochastic infection events, the infectious units per virus was increased to 5x the original amount. Therefore, for the eight virus competitions previously performed the infectious units per virus in each mixture was increased to 750 IU instead of 150 IU. With this increased MOI, the absolute abundance of integrated HIV-1 DNA in tissues (both cervix and foreskin, measured by qPCR) increased by 1.65-fold (**Figure 15**). Moreover, the PCR efficiency improved (**Figure 14B**) with an overall efficiency of 85-90%.

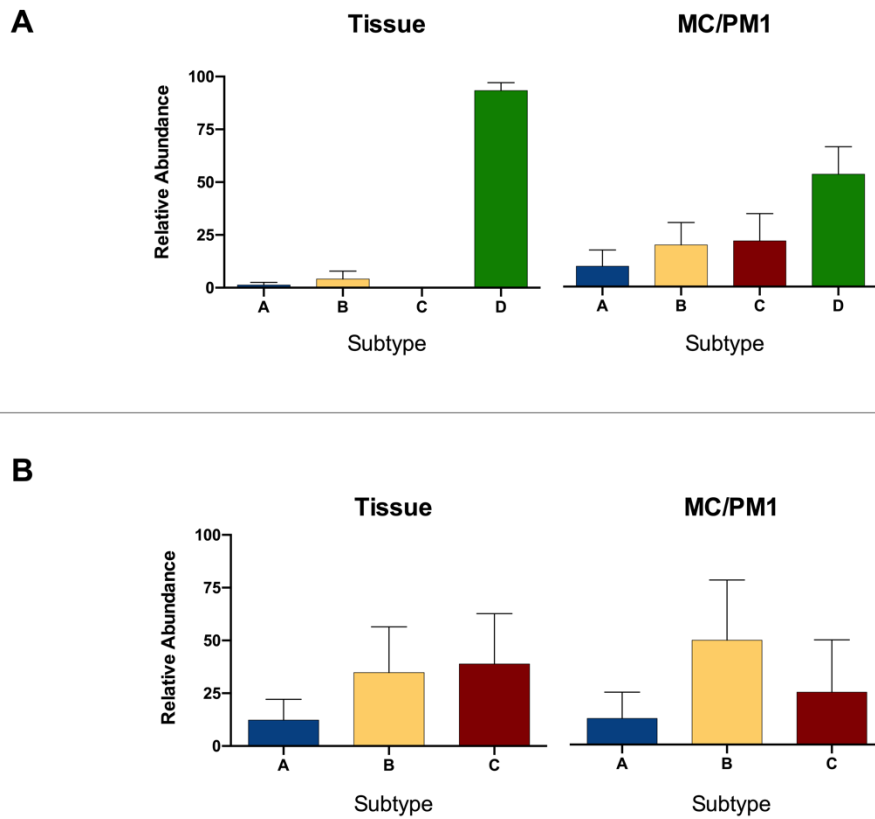


Figure 12. Average relative abundance of each subtype in cervical tissue and from migratory cells after infection at 0.01MOI

(A) Cervical tissue was dissected into $\sim 3\text{mm}^3$ explants and exposed to mixtures of 4 different *env* chimeric viruses at 150 IU each (repeated in $n=2$ tissue donors; 2 technical replicates of tissue and 2 of MC/PM1 per competition). The average relative abundance for each subtype is presented in tissue and MC/PM1 co-cultures. (A) Competitions including all four subtypes; (B) competitions excluding subtype D. Mean values with SEM are shown.

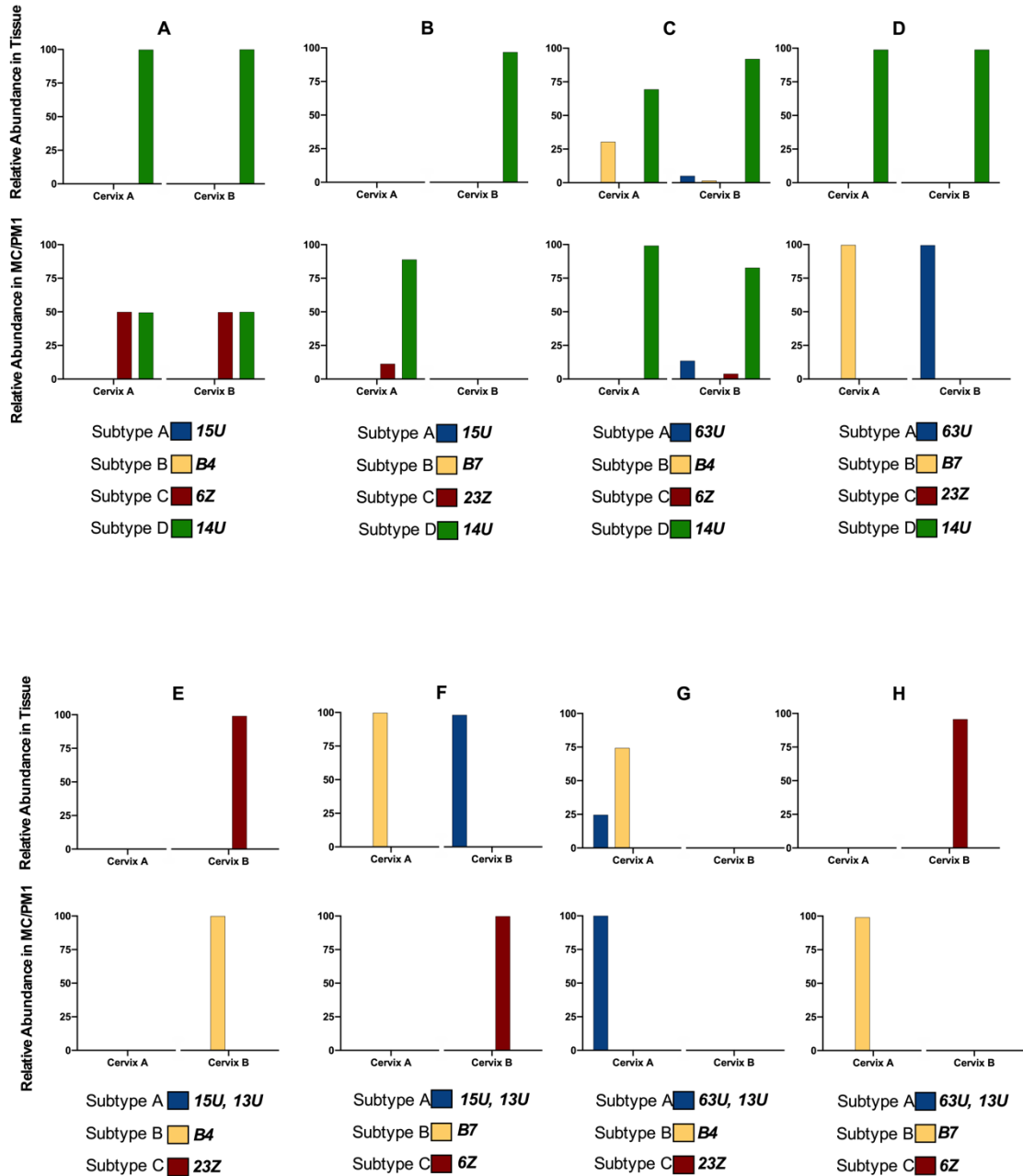


Figure 13. Individual multi-virus competitions using cervical tissue at 0.01 MOI, grouped by subtype.

(A-H) Cervical tissue (n=2) was dissected into $\sim 3\text{mm}^3$ explants and exposed to mixtures of 4 different *env* chimeric viruses as shown below the graphs. Competitions were

performed in duplicate. The average relative abundance for each subtype in each specific competition for cervical tissue and MC/PM1 co-cultures are presented.

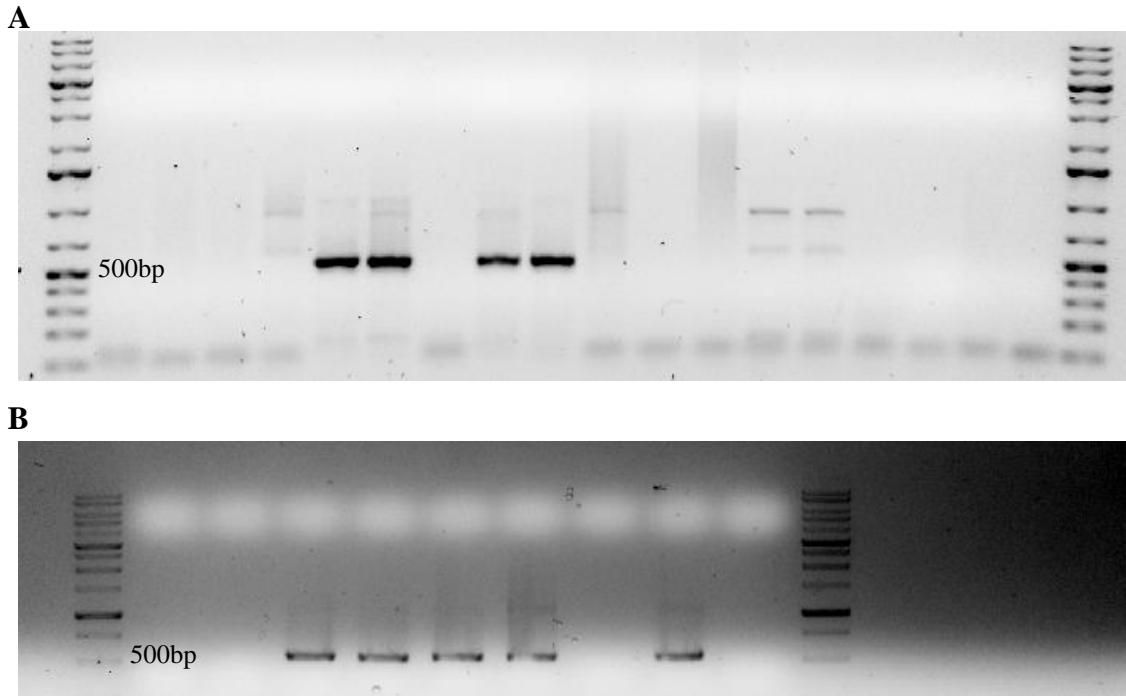


Figure 14. Two representative electrophoresis gels to demonstrate PCR efficiencies

(A) 1% agarose gels were used to determine the presence of C2-V3 *env* product at ~500bp. At 0.01 MOI, PCR efficiencies were low: out of 16 samples only 4 were positive. 100bp DNA ladder was used. (B) At 0.05 MOI, PCR efficiencies increased: out of 8 samples 5 were positive. 1kb DNA ladder used.

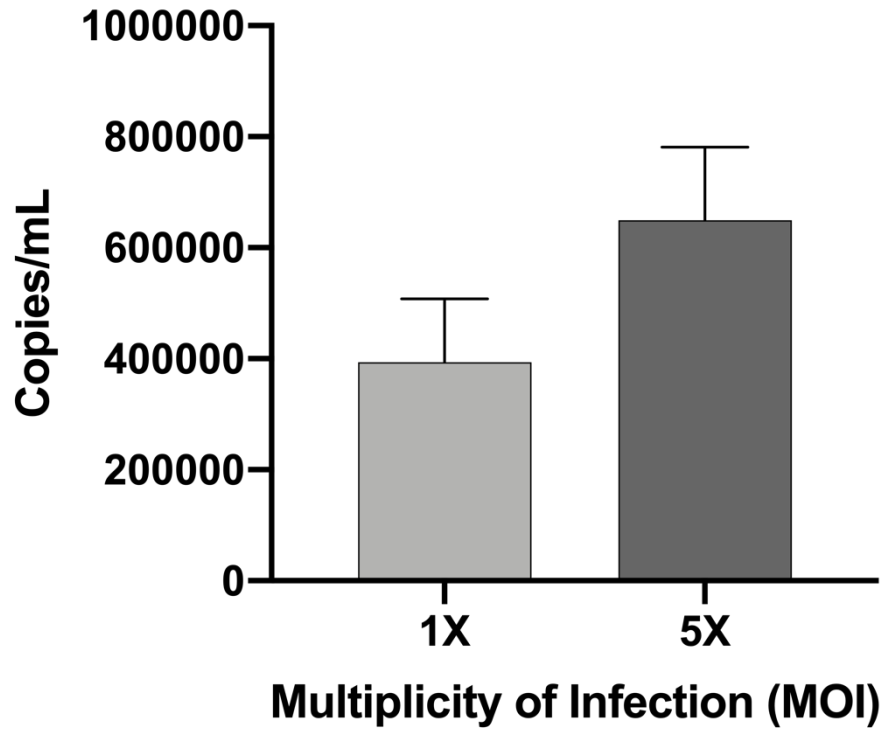


Figure 15. Comparison of absolute quantity of integrated HIV DNA in tissue between MOI conditions

Cervical tissue (n=2) exposed to 150IU or cervical (n=1) and foreskin (n=1) tissue exposed to 750IU of each virus were harvested after 10 days, tissue was lysed and total HIV-1 copy number between the two MOI conditions was assessed using a gag-specific qPCR. Mean with SEM values are shown.

3.4.2 Subtype Transmission Fitness Differences in Cervical Tissue

Figure 16 provides a summary that compares the average relative abundance of each subtype across all the competitions in cervical tissue, separating the same competitions that included all subtypes (Panel A) and those that did not include subtype D (Panel B). **Figure 17** provides the same data as **Figure 15**, but showing the results of each individual competition with viruses grouped by subtype (competitions performed in duplicate, average of replicates shown). The number of competitions with at least one replicate having an identified target sequence increased. Viral replication was not measured in only two competitions at 0.05 MOI in cervical tissue (**Figure 17E,G**) when compared to 5/8 competitions that did not measure viral replication in either tissue or MC/PM1 co-cultures at the 0.01 MOI (**Figures 13B, E-H**). The increased PCR efficiency coupled with the increased number of competitions with measurable viral replication provided more confidence that the trends exhibited in **Figure 16** were not due to stochastic infection events. Therefore at this MOI, the relative transmission fitness differences between the subtypes were evaluated.

When all four dominant group M subtypes were competed against each other, all the other subtypes were outcompeted by subtype D in the tissue except for subtype A, which had approximately 12.5% replication in the tissue (being observed in one replicate of one competition). Not only was there a high level of subtype D replication in the tissue, only subtype D was pulled through the tissue by MCs for replication in PM1 cells. Therefore, despite subtype D accounting for only 25% of the inoculating mixture, it was present in greater than 85% of replicating virus in the tissue and 100% of the virus being transmitted out of the tissue for replication in PM1 cells.

Due to the fact that subtype D virus 14U took over viral replication in the tissue and MC/PM1 co-cultures, transmission fitness differences between the other subtypes could not be discerned. Therefore, subtype D was eliminated from a subset of competitions to attempt to investigate the relative transmission fitness of the other subtypes. In the absence of subtype D virus, we observed trend differences in the transmission of subtypes A-C in cervical tissue (**Figure 16B**). Subtype C viruses had the highest level of replication in tissue compared to the other subtypes but were pulled through the tissue by MCs to replicate in PM1 cells the least efficiently. Subtype B viruses did not replicate in the tissue at all, but had the highest level of replication in MC/PM1 co-cultures; similarly, subtype A viruses had very low levels of replication in the tissue but had higher levels of replication than subtype C in MC/PM1 co-cultures.

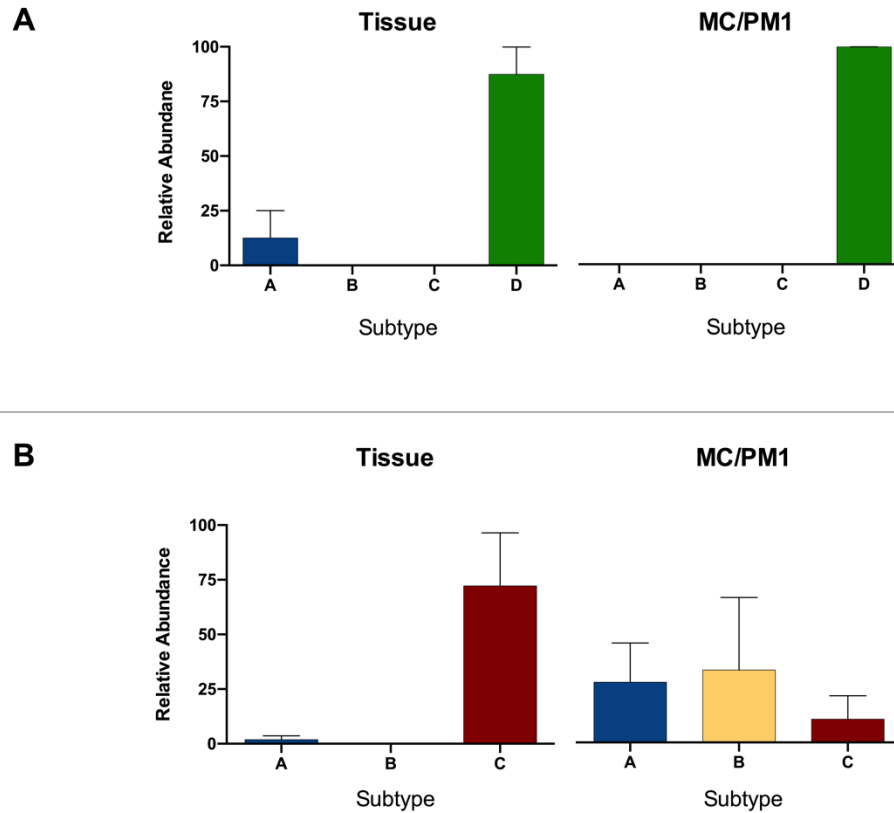


Figure 16. Average relative abundance of each subtype in cervical tissue and from migratory cells after infection at 0.05 MOI

Cervical tissue (n=1) was dissected into ~3mm³ explants and exposed to mixtures of 4 different *env* chimeric viruses at 750 IU each. The average relative abundance of each subtype across all eight competitions in tissue and MC/PM1 co-cultures are presented. Each competition was done in done in duplicate. **(A)** Competitions including all four subtypes; **(B)** competitions excluding subtype D virus. Mean values with SEM are shown.

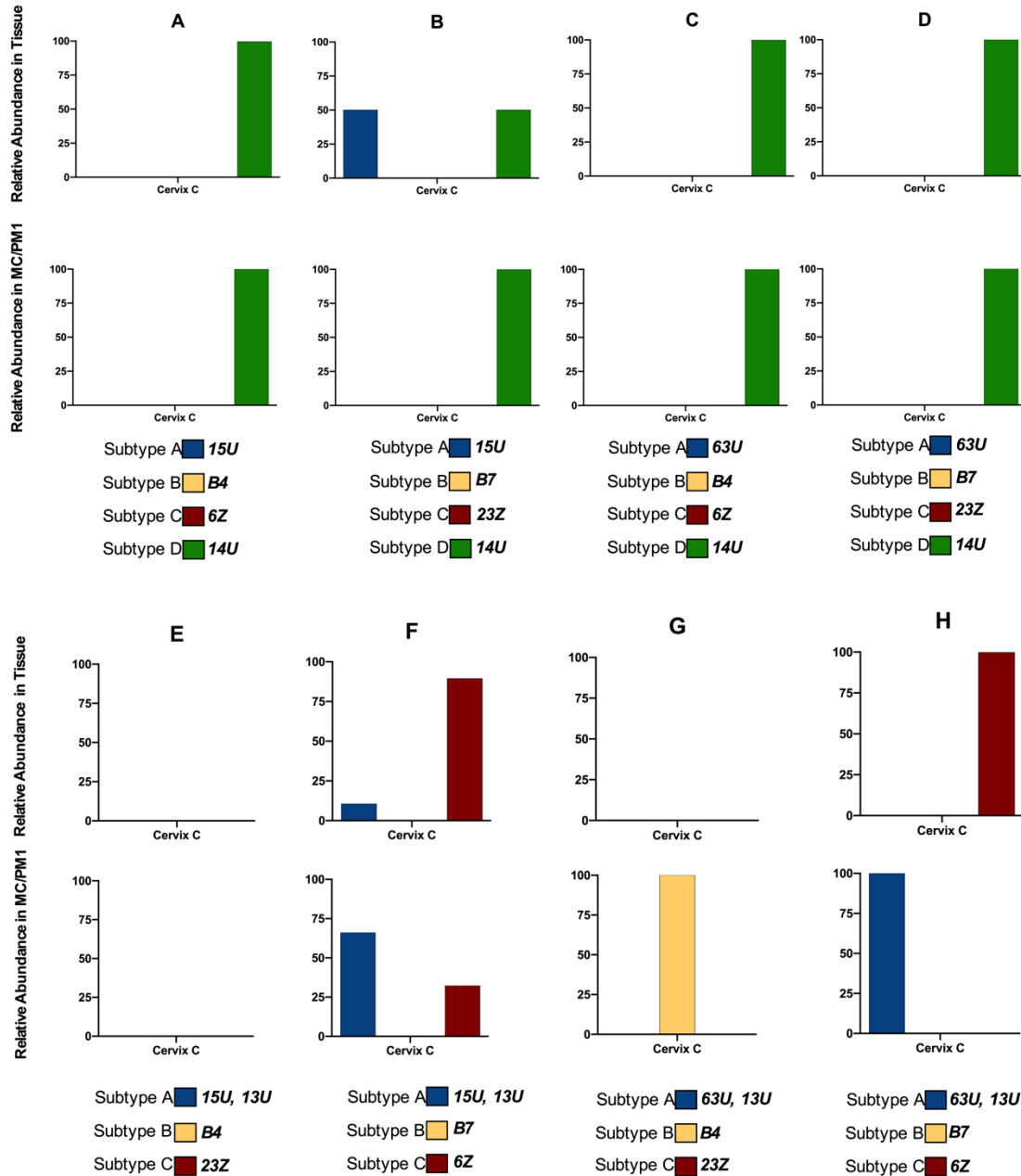


Figure 17. Individual multi-virus competitions using cervical tissue at 0.05 MOI, grouped by subtype

(A-H) Cervical explant tissue (n=1) was exposed to mixtures of 4 different *env* chimeric viruses as shown below the graphs. Competitions were performed in duplicate. The average

relative abundance for each subtype in each specific competition for tissue and MC/PM1 co-cultures are presented.

3.4.3 Subtype Transmission Fitness Differences in Foreskin Tissue

Trends in relative transmission fitness of HIV-1 subtypes were different in the foreskin compared to the cervix (**Figure 18**). Similarly to the cervix, subtype D once again outcompeted the other subtypes in the tissue. There was low levels of replication of subtypes B and C but no subtype A replication in the tissue. However, in contrast to the cervix, subtype B (as opposed to D) was pulled through foreskin tissue by MC's to infect PM1 cells the most efficiently. Subtype D accounted for only 25% of virus replication in the MC/PM1 co-cultures.

When foreskin tissue is infected with different subtypes in the absence of subtype D (**Figure 18B**), subtype B and C had equal levels of replication, ~43%, and subtype A had the lowest, at 7%. However, only subtype B viruses were observed in MC/PM1 co-cultures.

Figure 19 provides the same data as **Figure 18**, but showing the results of each individual competition with viruses grouped by subtype (competitions performed in duplicate, average of replicates shown). Unlike cervical tissue, viral replication was measured in both compartments in at least one replicate for all competitions performed in foreskin tissue.

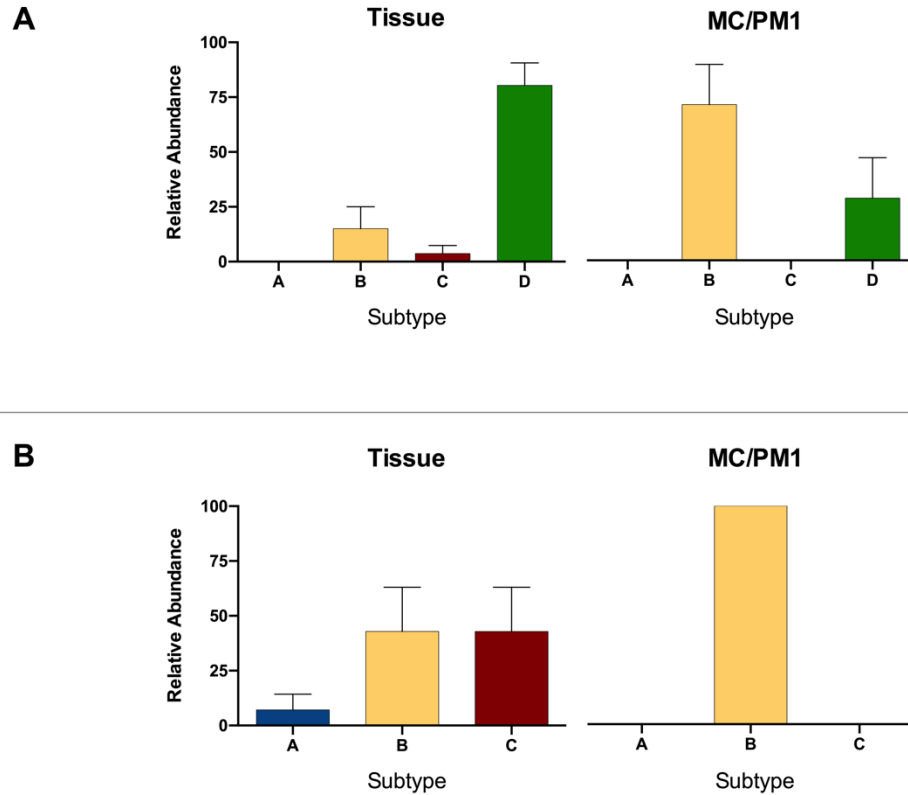


Figure 18. Average relative abundance of each subtype in foreskin tissue and from migratory cells after infection at 0.05 MOI

Foreskin tissue (n=1) was dissected into $\sim 3\text{mm}^3$ explants and exposed to mixtures of 4 different *env* chimeric viruses at 750 IU each. The average relative abundance of each subtype across all eight competitions in tissue and MC/PM1 co-cultures are presented. Each competition was done in duplicate. **(A)** Competitions including all four subtypes; **(B)** competitions excluding subtype D virus. Mean values with SEM are shown.

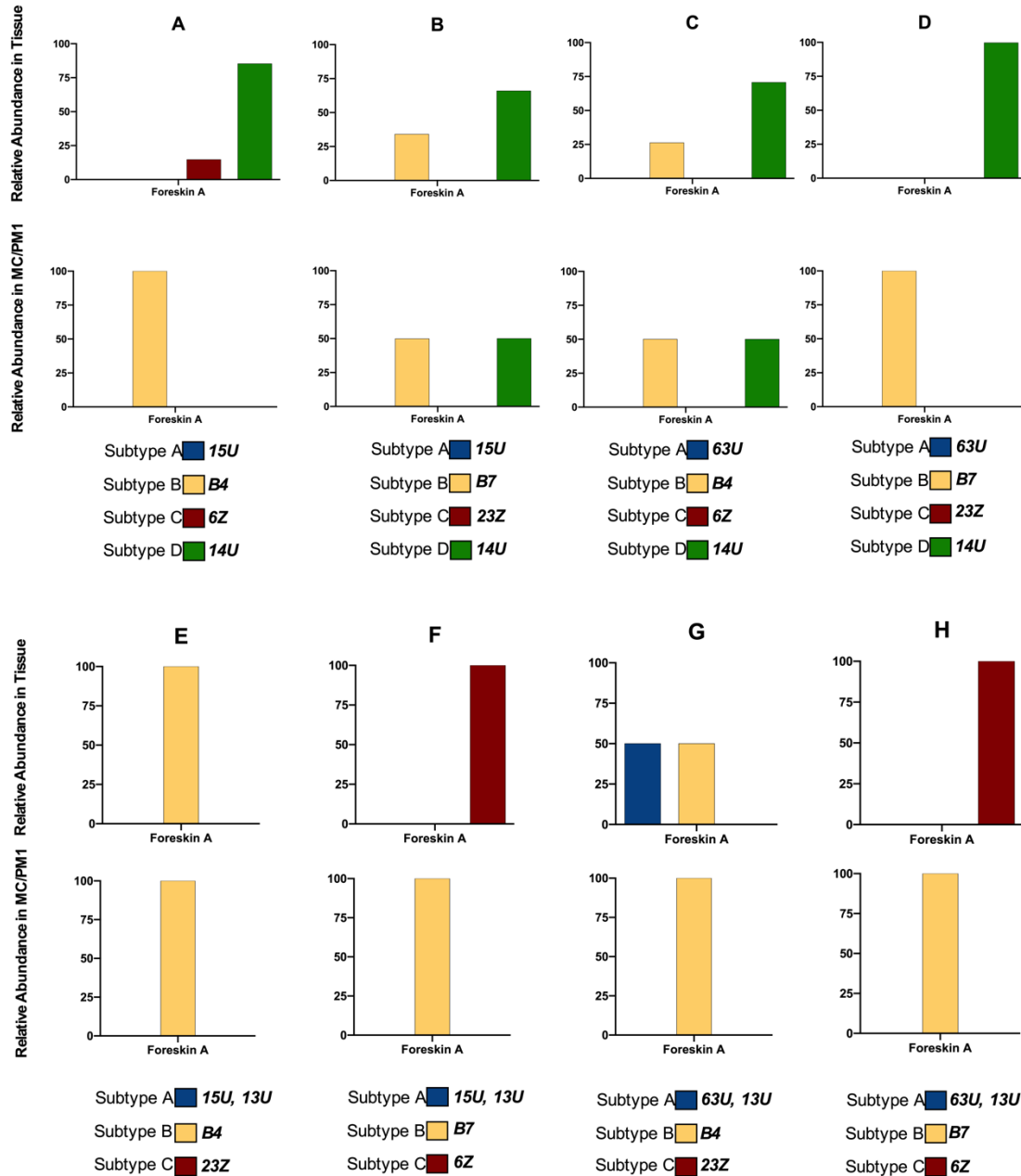


Figure 19. Individual multi-virus competitions using foreskin tissue at 0.05 MOI, grouped by subtype

(A-H) Foreskin explant tissue (n=1) was exposed to mixtures of 4 different *env* chimeric viruses as shown below the graphs. Competitions were performed in duplicate. The average

relative abundance for each subtype in each specific competition for tissue and MC/PM1 co-cultures are presented.

3.5 Relative Abundance of each Individual Virus in Cervical and Foreskin Tissue

In summary, in cervical tissue the trends suggest that subtype D is the most effective at replicating in the tissue and being pulled through by MCs for replication in PM1 cells. Once subtype D is removed, the trends suggest that subtype B is pulled through the tissue the most efficiently, followed by subtypes A and C, respectively. This trend was observed despite the fact that subtype C replicated in the tissue the most effectively.

When viruses from all four subtypes were competed against one another, subtype A virus 15U and subtype D virus 14U were solely responsible for the trends stated above (**Figure 20A**). These specific viruses drove the trends that suggest subtype D replicates in the tissue and MC/PM1 co-cultures the most effectively.

In the absence of subtype D, the relative transmission of subtypes B and C were driven by one virus of each subtype (**Figure 20B**). Viruses B4 and 6Z were solely responsible for the trends observed for subtypes B and C, respectively. Two viruses, 63U and 13U, were responsible for the trends observed for subtype A, and there was no measured replication of virus 15U in MC/PM1 co-cultures. Subtype C virus 6Z outcompeted the other viruses in the tissue.

In foreskin tissue, the trends suggest that subtype D is the most effective at replicating in the tissue but subtype B is the most effective at replicating in MC/PM1 co-cultures, even in the presence of subtype D. We observed in all eight competitions the relative transmission of subtype B was driven by both B4 and B7 (**Figure 21A,B**). Otherwise, any

replication observed for the other subtypes A, C, and D, were driven by one virus respectively: 13U, 6Z, and 14U (**Figure 21A,B**).

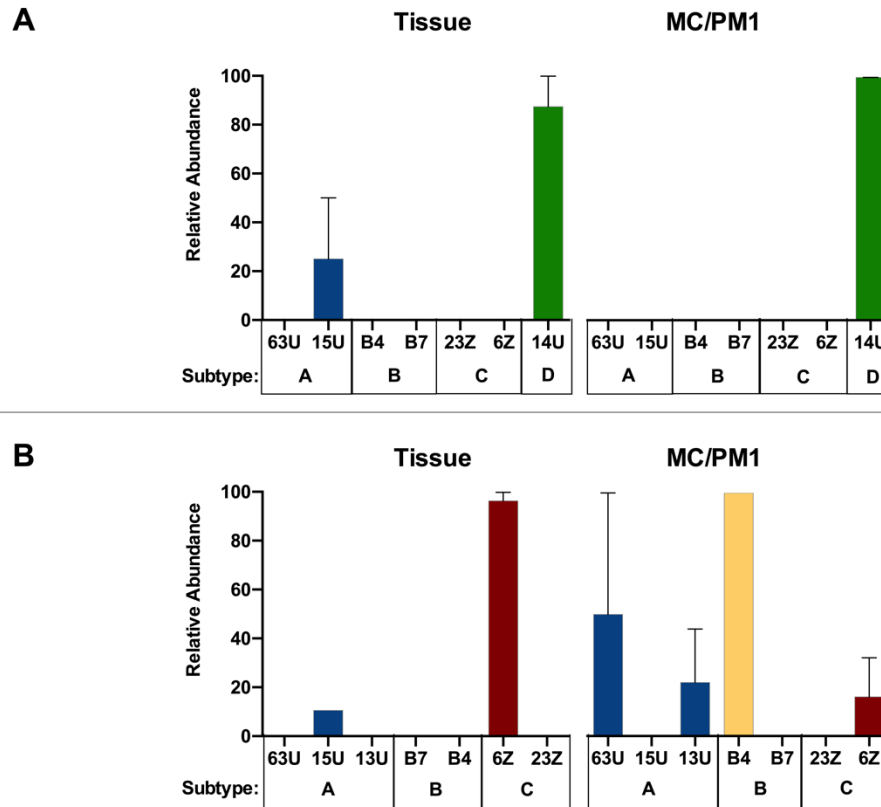


Figure 20. Average relative abundance of each individual virus in cervical tissue at 0.05 MOI

Cervical tissue (n=1) was dissected into ~3mm³ explants and exposed to mixtures of 4 different *env* chimeric viruses at 750 IU each. The average relative abundance for each specific virus across all eight competitions in tissue and MC/PM1 co-cultures are presented. Each competition was done in done in duplicate. **(A)** Competitions including all four subtypes; **(B)** competitions excluding subtype D. Mean values with SEM are shown.

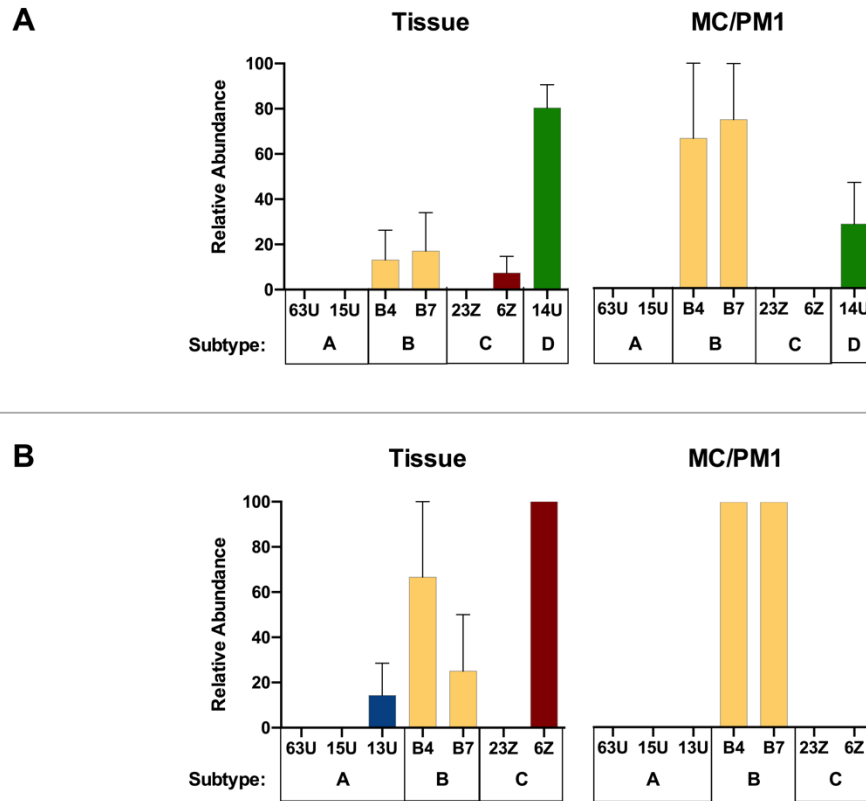


Figure 21. Average relative abundance of each individual virus in foreskin tissue at 0.05 MOI

Foreskin tissue (n=1) was dissected into $\sim 3\text{mm}^3$ explants and exposed to mixtures of 4 different *env* chimeric viruses at 750 IU each. The average relative abundance for each specific virus across all eight competitions in tissue and MC/PM1 co-cultures are presented. Each competition was done in duplicate. **(A)** Competitions including all four subtypes; **(B)** competitions excluding subtype D. Mean values with SEM are shown.

Chapter 4: Discussion and Conclusion

When comparing the pathogenicity of the dominant HIV-1 group M subtypes, patients infected with HIV-1 subtype C progress to AIDS at a slower rate and consequently have lower mortality rates compared to those infected with the other subtypes⁹⁰. Disease progression is driven by the repeated infection and killing of CD4+ T cells, leading to gradual exhaustion and loss of this cell type. Evidence supports the notion that a virus' ability to replicate *in vitro* in PBMCs or CD4+ T cells is a predictor of their effect on disease progression in the host^{78-80,84}. Consistent with this, previous studies by our group performed pairwise competitions of HIV-1 subtypes in PBMCs or CD4+ T cells and revealed subtype C to have the lowest replicative ability^{55,82}. In fact, these competitions revealed a general pathogenic fitness order of $D = B > A > C$ ^{55,90}. Thus, it is possible that HIV-1 subtype C is dominating the epidemic due to increased opportunities for infection. With 2-5 more years of asymptomatic disease⁹⁰, the infected host can transmit the virus more frequently. However, the ability for a virus to replicate in blood cells and cause rapid disease progression may or may not be related to its ability to efficiently infect genital mucosa and thus transmit efficiently. Both opportunity for infection and transmission efficiency are key factors of pathogen survival.

In this study, I investigated the ability of four dominant group M subtypes, subtypes A, B, C, and D, to infect genital mucosal tissue as a measure of transmission efficiency. Transmission fitness was assessed through both a) direct infection of tissue resident susceptible cell populations and local replication; and b) uptake of the virus by tissue resident cells that migrate out of the tissue to infect cells elsewhere in the body (i.e. draining lymph nodes) for systemic infection. Using this model, I found that subtype D viruses

outcompeted the other subtypes in both foreskin and cervical tissue. However, while subtype D was also efficiently taken up and disseminated by cells migrating out of the cervix, subtype B viruses were more efficient at this process in foreskin tissue. This was in contrast to simple replicative fitness in CD4+ PM1 cells, where subtype D was far more efficient at replicating than the other subtypes. Through this study, I confirmed the results of previous reports indicating subtype C has lower replicative fitness than subtype D. However, I did not observe that HIV-1 subtype C had even comparable, let alone greater transmission efficiency than the other subtypes. My data suggests that the gradually increasing prevalence and transmission of subtype C observed globally is not due to inherent increased transmission fitness of subtype C viruses. Instead, subtype C's dominance of the epidemic may be due to its decreased pathogenicity, allowing infected individuals more years between HIV seroconversion and the onset of AIDS symptoms during which they may transmit the virus. In the long history of SIV infection in African nonhuman primates, SIV and its natural hosts have evolved together resulting in the host showing no signs of SIV-induced disease or simian AIDS^{108,109}. Although highly speculative, HIV-1 subtype C and the human host could be exhibiting a similar phenomenon where its adaptation to the host has led it to have decreased pathogenicity. For HIV-1 subtype B and D, their increased pathogenicity leads to faster disease progression and mortality. Higher transmission fitness may compensate for this increased replicative fitness. With less opportunity for infection, perhaps these subtypes evolved to increase their transmission efficiency in order to survive and persist.

As described above, when viruses are competed directly on a susceptible CD4+ T cell line (PM1 cells), it is predictive of *in vivo* pathogenic fitness and disease progression. Our

results in PM1 cells are comparable to the general fitness order determined in PBMCs^{55,82}, where subtype D and subtype B replicate more effectively than subtypes A and C. However, in my study, subtype D outcompeted subtype B, accounting for over 80% of viral replication in directly infected PM1 cells, in contrast to previous reports where subtype B and D viruses were more evenly matched. Moreover, in competitions that did not include subtype D I did not observe any difference in replicative fitness between subtypes A, B and C.

The main limitation of my study is the utilization of only one subtype D virus, and only 2-3 viruses used for the other subtypes. By increasing the diversity of viruses within a subtype, future studies will be able to more precisely attribute the results to actual subtype differences. This may also be the reason for why there were no replicative fitness differences between subtypes A, B, and C in the direct PM1 competitions. It is possible that 14U is a particularly strong virus and doesn't accurately represent subtype D as a whole. Additionally, when analyzing the average replication of each individual virus, in foreskin tissue the trends seen for subtypes A and C depended only on viruses 13U and 6Z, respectively. During propagation of different subtype D viruses, only 14U was able to infect U87.CD4.CCR5 cells and be produced at a titre high enough to be used in transmission experiments. As such, future studies may need to re-insert the *env* gene from the different subtype D primary viruses into the pREC_nfl_{NL4-3}Δenv backbone, and should include more representative viruses of each subtype in these competitions.

Nonetheless, my results are consistent with viral replication in PM1 cells being similar to viral replication measured in both cervical and foreskin tissue. Although the relative

transmission fitness differences between the other subtypes could not be discerned, subtype D was the most effective at replicating in the tissue and in direct competitions on PM1 cells. These studies need to be repeated with more representative viruses from each subtype, but the pathogenic fitness of a virus may be able to predict its replication ability in genital tissue.

In foreskin tissue, transmission of HIV-1 by migratory cells to PM1 cells does not follow the trends seen in direct competitions on PM1 cells. Although subtype D was the most effective at replicating in the tissue, subtype B was more efficiently taken up and disseminated by cells migrating out of the foreskin. As demonstrated *in vitro*, cell-to-cell transfer of HIV-1 is 100-1000 fold more efficient than infection carried out by cell-free viral particles³⁴⁻³⁸. It has been argued that cell-to-cell transmission of HIV-1 is the main route of transmission *in vivo*^{39,40}, but the role that cell-to-cell vs. cell-free transmission plays is still up for debate. However, the fact that the subtype most effective at replicating in foreskin tissue is not the same subtype that is the most efficient at being transported to PM1 cells is important. Thus, we need to consider these migrating cells in the context of sexual transmission of HIV-1. Utilizing genital tissue in these investigations creates a more complete picture of transmission events. Exclusively looking at replication in PM1 cells may only represent a virus' ability to infect and replicate in tissue resident cell populations.

Previous competition experiments in tissue explants demonstrate that there is a clear “winner” as measured by one virus establishing the majority of viral replication in either tissue or MC/PM1^{55,82}. As mentioned, it seems that in this model once a given virus has the opportunity for infection in the tissue and/or migration out of the tissue to susceptible

cells, the virus takes over and the majority of viral replication is attributed to that one virus. This was the reason for the round-robin design of the competitions. In our study, when tissue was infected with 150 IU of each virus this phenomenon was not clearly observed. By examining the individual multi-virus competitions, viral replication was not measured in 5/8 competitions, and the absence of viral replication was observed in at least one donor for all four of the competitions lacking a subtype D virus. Additionally, when a virus did establish infection the “winning” virus was not reproducible between competitions. With an overall PCR efficiency of 45-50%, there was a high possibility that any trends in transmission fitness observed were due to random infection events where true fitness differences could not be confidently deduced. To rectify this issue, I increased the number of infectious units to 750, 5x the original amount. With this increased MOI, I obtained higher PCR amplification efficiencies (85-90%) and measurable viral replication in all but two competitions in cervical tissue. This study helps refine the *ex vivo* explant assay and its requirement for a greater number of infectious units to yield more consistent and potentially more translatable results. The exact mechanism behind the increased number of infectious units being a necessity still needs to be elucidated.

In conclusion, our trends suggest that HIV-1 subtype D dominates viral replication in the tissue and is the most efficient at migrating out of the cervix for infection in PM1 cells. However, in foreskin tissue the effect of migratory cells on subtype transmission may be different than that of the cervix. Regardless, HIV-1 subtype C does not seem to have a higher transmission fitness in the presence of the other subtypes. A virus' pathogenic fitness may be predictive of its ability to infect and replicate in tissue-resident susceptible cell populations, however studies that include more representative viruses from each

subtype will need to be done to confirm these results. The high prevalence of HIV-1 subtype C in the epidemic may be due to adaptation of the virus to the host and the faster disease progression of subtypes B and D may require higher transmission efficiencies to maintain itself in the HIV epidemic. Overall, to design effective vaccine strategies there is a need to identify a phenotype of HIV-1 that is transmitted more favourably. At least in foreskin tissue, the subtype that is transported to susceptible cells is different than the subtype that replicates the most effectively in tissue. Therefore, we must continue to use genital tissues in sexual transmission studies to more precisely understand transmission events in the mucosa.

References

1. Gallo, R. C. *et al.* Isolation of human T-cell leukemia virus in acquired immune deficiency syndrome (AIDS). *Science* **220**, 865–7 (1983).
2. Barre-Sinoussi, F. *et al.* Isolation of a T-lymphotropic retrovirus from a patient at risk for acquired immune deficiency syndrome (AIDS). *Science* (80-.). **220**, 868–871 (1983).
3. UNAID. Fact Sheet - Global AIDS Update 2019. 1–6 (2019).
4. WHO | HIV/AIDS. *WHO* (2018).
5. Shaw, G. M. & Hunter, E. HIV transmission. *Cold Spring Harb. Perspect. Med.* **2**, a006965 (2012).
6. del Rio, C. The global HIV epidemic: What the pathologist needs to know. *Semin. Diagn. Pathol.* **34**, 314–317 (2017).
7. Taylor, B. S., Sobieszczyk, M. E., McCutchan, F. E. & Hammer, S. M. The Challenge of HIV-1 Subtype Diversity. *N. Engl. J. Med.* **358**, 1590–1602 (2008).
8. Lever, A. M. L. HIV: the virus. *Medicine (Baltimore)*. **37**, 313–316 (2009).
9. Van Heuverswyn, F. *et al.* SIV infection in wild gorillas. *Nature* **444**, 164–164 (2006).
10. Keele, B. F. *et al.* Chimpanzee reservoirs of pandemic and nonpandemic HIV-1. *Science* **313**, 523–6 (2006).
11. Ayouba, A. *et al.* HIV-1 group O infection in Cameroon, 1986 to 1998. *Emerg. Infect. Dis.* **7**, 466–7 (2001).
12. Essex, M. Human immunodeficiency viruses in the developing world. *Adv. Virus Res.* **53**, 71–88 (1999).
13. Burke, D. S. Recombination in HIV: an important viral evolutionary strategy. *Emerg. Infect. Dis.* **3**, 253–9 (1997).
14. NIH. HIV Databases. (2019). Available at: <https://www.hiv.lanl.gov/content/index>. (Accessed: 20th June 2019)
15. Haase, A. T. Targeting early infection to prevent HIV-1 mucosal transmission. *Nature* **464**, 217–223 (2010).
16. Gray, R. H. *et al.* Probability of HIV-1 transmission per coital act in monogamous, heterosexual, HIV-1-discordant couples in Rakai, Uganda. *Lancet (London, England)* **357**, 1149–53 (2001).
17. Wawer, M. J. *et al.* Rates of HIV-1 transmission per coital act, by stage of HIV-1 infection, in Rakai, Uganda. *J. Infect. Dis.* **191**, 1403–9 (2005).
18. Quinn, T. C. *et al.* Viral Load and Heterosexual Transmission of Human Immunodeficiency Virus Type 1. *N. Engl. J. Med.* **342**, 921–929 (2000).
19. Barreiro, P. *et al.* Natural pregnancies in HIV-serodiscordant couples receiving successful antiretroviral therapy. *J. Acquir. Immune Defic. Syndr.* **43**, 324–6 (2006).
20. Castilla, J. *et al.* Effectiveness of highly active antiretroviral therapy in reducing heterosexual transmission of HIV. *J. Acquir. Immune Defic. Syndr.* **40**, 96–101 (2005).
21. Carias, A. M. *et al.* Defining the Interaction of HIV-1 with the Mucosal Barriers of the Female Reproductive Tract. *J. Virol.* **87**, 11388–11400 (2013).
22. Sturm-Ramirez, K., Gaye-Diallo, A., Eisen, G., Mboup, S. & Kanki, P. J. High

- levels of tumor necrosis factor-alpha and interleukin-1beta in bacterial vaginosis may increase susceptibility to human immunodeficiency virus. *J. Infect. Dis.* **182**, 467–73 (2000).
23. Greenhead, P. *et al.* Parameters of Human Immunodeficiency Virus Infection of Human Cervical Tissue and Inhibition by Vaginal Virucides. *J. Virol.* **74**, 5577–5586 (2000).
 24. Prodger, J. L. *et al.* Chemokine Levels in the Penile Coronal Sulcus Correlate with HIV-1 Acquisition and Are Reduced by Male Circumcision in Rakai, Uganda. *PLoS Pathog.* **12**, e1006025 (2016).
 25. Narimatsu, R., Wolday, D. & Patterson, B. K. IL-8 Increases Transmission of HIV Type 1 in Cervical Explant Tissue. *AIDS Res. Hum. Retroviruses* **21**, 228–233 (2005).
 26. Masson, L. *et al.* Genital Inflammation and the Risk of HIV Acquisition in Women. *Clin. Infect. Dis.* **61**, 260–269 (2015).
 27. Zaitseva, M. *et al.* Expression and function of CCR5 and CXCR4 on human Langerhans cells and macrophages: implications for HIV primary infection. *Nat. Med.* **3**, 1369–75 (1997).
 28. Gupta, P. *et al.* Memory CD4+ T Cells Are the Earliest Detectable Human Immunodeficiency Virus Type 1 (HIV-1)-Infected Cells in the Female Genital Mucosal Tissue during HIV-1 Transmission in an Organ Culture System. *J. Virol.* **76**, 9868–9876 (2002).
 29. Meng, G. *et al.* Primary intestinal epithelial cells selectively transfer R5 HIV-1 to CCR5+ cells. *Nat. Med.* **8**, 150–156 (2002).
 30. Asin, S. N., Eszterhas, S. K., Rollenhagen, C., Heimberg, A. M. & Howell, A. L. HIV type 1 infection in women: increased transcription of HIV type 1 in ectocervical tissue explants. *J. Infect. Dis.* **200**, 965–72 (2009).
 31. Patterson, B. K. *et al.* Detection of HIV-1 DNA and messenger RNA in individual cells by PCR-driven in situ hybridization and flow cytometry. *Science* **260**, 976–9 (1993).
 32. Coombs, R. W. *et al.* Lower genitourinary tract sources of seminal HIV. *J. Acquir. Immune Defic. Syndr.* **41**, 430–8 (2006).
 33. Mostad, S. B. & Kreiss, J. K. Shedding of HIV-1 in the genital tract. *AIDS* **10**, 1305–15 (1996).
 34. Phillips, D. M. The role of cell-to-cell transmission in HIV infection. *AIDS* **8**, 719–732 (1994).
 35. Dimitrov, D. S., Broder, C. C., Berger, E. A. & Blumenthal, R. Calcium ions are required for cell fusion mediated by the CD4-human immunodeficiency virus type 1 envelope glycoprotein interaction. *J. Virol.* **67**, 1647–52 (1993).
 36. Carr, J. M., Hocking, H., Li, P. & Burrell, C. J. Rapid and efficient cell-to-cell transmission of human immunodeficiency virus infection from monocyte-derived macrophages to peripheral blood lymphocytes. *Virology* **265**, 319–29 (1999).
 37. Chen, P., Hübner, W., Spinelli, M. A. & Chen, B. K. Predominant mode of human immunodeficiency virus transfer between T cells is mediated by sustained Env-dependent neutralization-resistant virological synapses. *J. Virol.* **81**, 12582–95 (2007).
 38. Martin, N. & Sattentau, Q. Cell-to-cell HIV-1 spread and its implications for

- immune evasion. *Curr. Opin. HIV AIDS* **4**, 143–149 (2009).
39. Zhong, P., Agosto, L. M., Munro, J. B. & Mothes, W. Cell-to-cell transmission of viruses. *Curr. Opin. Virol.* **3**, 44–50 (2013).
 40. Sourisseau, M., Sol-Foulon, N., Porrot, F., Blanchet, F. & Schwartz, O. Inefficient Human Immunodeficiency Virus Replication in Mobile Lymphocytes. *J. Virol.* **81**, 1000–1012 (2007).
 41. McCoombe, S. G. & Short, R. V. Potential HIV-1 target cells in the human penis. *AIDS* **20**, 1491–1495 (2006).
 42. Shen, R. *et al.* Vaginal myeloid dendritic cells transmit founder HIV-1. *J. Virol.* **88**, 7683–8 (2014).
 43. Fahrback, K. M. *et al.* Activated CD34-derived Langerhans cells mediate transinfection with human immunodeficiency virus. *J. Virol.* **81**, 6858–68 (2007).
 44. Cameron, P. U. *et al.* Dendritic cells exposed to human immunodeficiency virus type-1 transmit a vigorous cytopathic infection to CD4+ T cells. *Science* **257**, 383–7 (1992).
 45. Geijtenbeek, T. B. *et al.* DC-SIGN, a dendritic cell-specific HIV-1-binding protein that enhances trans-infection of T cells. *Cell* **100**, 587–97 (2000).
 46. Ping, L.-H. *et al.* Comparison of viral Env proteins from acute and chronic infections with subtype C human immunodeficiency virus type 1 identifies differences in glycosylation and CCR5 utilization and suggests a new strategy for immunogen design. *J. Virol.* **87**, 7218–33 (2013).
 47. Joseph, S. B. *et al.* Quantification of entry phenotypes of macrophage-tropic HIV-1 across a wide range of CD4 densities. *J. Virol.* **88**, 1858–69 (2014).
 48. Parrish, N. F. *et al.* Transmitted/founder and chronic subtype C HIV-1 use CD4 and CCR5 receptors with equal efficiency and are not inhibited by blocking the integrin $\alpha 4\beta 7$. *PLoS Pathog.* **8**, e1002686 (2012).
 49. Hu, Q. *et al.* Blockade of attachment and fusion receptors inhibits HIV-1 infection of human cervical tissue. *J. Exp. Med.* **199**, 1065–75 (2004).
 50. Hladik, F. *et al.* Initial events in establishing vaginal entry and infection by human immunodeficiency virus type-1. *Immunity* **26**, 257–70 (2007).
 51. Tobian, A. A. R., Kacker, S. & Quinn, T. C. Male Circumcision: A Globally Relevant but Under-Utilized Method for the Prevention of HIV and Other Sexually Transmitted Infections. *Annu. Rev. Med.* **65**, 293–306 (2014).
 52. McKinnon, L. R. & Kaul, R. Quality and quantity. *Curr. Opin. HIV AIDS* **7**, 195–202 (2012).
 53. McKinnon, L. R. *et al.* Characterization of a human cervical CD4+ T cell subset coexpressing multiple markers of HIV susceptibility. *J. Immunol.* **187**, 6032–42 (2011).
 54. Gosselin, A. *et al.* Peripheral blood CCR4+CCR6+ and CXCR3+CCR6+CD4+ T cells are highly permissive to HIV-1 infection. *J. Immunol.* **184**, 1604–16 (2010).
 55. Abraha, A. *et al.* CCR5- and CXCR4-Tropic Subtype C Human Immunodeficiency Virus Type 1 Isolates Have a Lower Level of Pathogenic Fitness than Other Dominant Group M Subtypes: Implications for the Epidemic. *J. Virol.* **83**, 5592–5605 (2009).
 56. McCoombe, S. G. & Short, R. V. Potential HIV-1 target cells in the human penis. *AIDS* **20**, 1491–1495 (2006).

57. Patterson, B. K. *et al.* Susceptibility to Human Immunodeficiency Virus-1 Infection of Human Foreskin and Cervical Tissue Grown in Explant Culture. *Am. J. Pathol.* **161**, 867–873 (2002).
58. Donoval, B. A. *et al.* HIV-1 target cells in foreskins of African men with varying histories of sexually transmitted infections. *Am. J. Clin. Pathol.* **125**, 386–91 (2006).
59. Abrahams, M.-R. *et al.* Quantitating the multiplicity of infection with human immunodeficiency virus type 1 subtype C reveals a non-poisson distribution of transmitted variants. *J. Virol.* **83**, 3556–67 (2009).
60. Keele, B. F. *et al.* Identification and characterization of transmitted and early founder virus envelopes in primary HIV-1 infection. *Proc. Natl. Acad. Sci. U. S. A.* **105**, 7552–7 (2008).
61. Byrn, R. A., Zhang, D., Eyre, R., McGowan, K. & Kiessling, A. A. HIV-1 in semen: an isolated virus reservoir. *Lancet* **350**, 1141 (1997).
62. Coombs, R. W. *et al.* Association between culturable human immunodeficiency virus type 1 (HIV-1) in semen and HIV-1 RNA levels in semen and blood: evidence for compartmentalization of HIV-1 between semen and blood. *J. Infect. Dis.* **177**, 320–30 (1998).
63. Gupta, P. *et al.* Human immunodeficiency virus type 1 shedding pattern in semen correlates with the compartmentalization of viral Quasi species between blood and semen. *J. Infect. Dis.* **182**, 79–87 (2000).
64. Zhu, T. *et al.* Genetic characterization of human immunodeficiency virus type 1 in blood and genital secretions: evidence for viral compartmentalization and selection during sexual transmission. *J. Virol.* **70**, 3098–107 (1996).
65. Joseph, S. B., Swanstrom, R., Kashuba, A. D. M. & Cohen, M. S. Bottlenecks in HIV-1 transmission: insights from the study of founder viruses. *Nat. Rev. Microbiol.* **13**, 414–25 (2015).
66. Keele, B. F. *et al.* Identification and characterization of transmitted and early founder virus envelopes in primary HIV-1 infection. *Proc. Natl. Acad. Sci. U. S. A.* **105**, 7552–7 (2008).
67. Klein, K. *et al.* Higher sequence diversity in the vaginal tract than in blood at early HIV-1 infection. *PLoS Pathog.* **14**, e1006754 (2018).
68. Berger, E. A., Murphy, P. M. & Farber, J. M. Chemokine receptors as HIV-1 coreceptors: roles in viral entry, tropism, and disease. *Annu. Rev. Immunol.* **17**, 657–700 (1999).
69. Zhu, T. *et al.* Genetic characterization of human immunodeficiency virus type 1 in blood and genital secretions: evidence for viral compartmentalization and selection during sexual transmission. *J. Virol.* **70**, 3098–107 (1996).
70. Roos, M. T. L. *et al.* Viral Phenotype and Immune Response in Primary Human Immunodeficiency Virus Type 1 Infection. *J. Infect. Dis.* **165**, 427–432 (1992).
71. Wilen, C. B., Tilton, J. C. & Doms, R. W. HIV: Cell Binding and Entry. *Cold Spring Harb. Perspect. Med.* **2**, a006866–a006866 (2012).
72. Sagar, M., Wu, X., Lee, S. & Overbaugh, J. Human immunodeficiency virus type 1 V1-V2 envelope loop sequences expand and add glycosylation sites over the course of infection, and these modifications affect antibody neutralization sensitivity. *J. Virol.* **80**, 9586–98 (2006).

73. Nawaz, F. *et al.* The genotype of early-transmitting HIV gp120s promotes α (4) β (7)-reactivity, revealing α (4) β (7) +/CD4+ T cells as key targets in mucosal transmission. *PLoS Pathog.* **7**, e1001301 (2011).
74. Go, E. P. *et al.* Characterization of Glycosylation Profiles of HIV-1 Transmitted/Founder Envelopes by Mass Spectrometry. *J. Virol.* **85**, 8270–8284 (2011).
75. Behrens, A.-J. *et al.* Composition and Antigenic Effects of Individual Glycan Sites of a Trimeric HIV-1 Envelope Glycoprotein. *Cell Rep.* **14**, 2695–706 (2016).
76. Coss, K. P. *et al.* HIV-1 Glycan Density Drives the Persistence of the Mannose Patch within an Infected Individual. *J. Virol.* **90**, 11132–11144 (2016).
77. Doores, K. J. *et al.* Envelope glycans of immunodeficiency virions are almost entirely oligomannose antigens. *Proc. Natl. Acad. Sci. U. S. A.* **107**, 13800–5 (2010).
78. Daniel, M., Kirchhoff, F., Czajak, S., Sehgal, P. & Desrosiers, R. Protective effects of a live attenuated SIV vaccine with a deletion in the nef gene. *Science (80-.).* **258**, 1938–1941 (1992).
79. Deacon, N. J. *et al.* Genomic Structure of an Attenuated Quasi Species of HIV-1 from a Blood Transfusion Donor and Recipients. *Science (80-.).* **270**, 988–991 (1995).
80. Kirchhoff, F., Greenough, T. C., Brettler, D. B., Sullivan, J. L. & Desrosiers, R. C. Brief report: absence of intact nef sequences in a long-term survivor with nonprogressive HIV-1 infection. *N. Engl. J. Med.* **332**, 228–32 (1995).
81. Abraha, A. *et al.* CCR5- and CXCR4-tropic subtype C human immunodeficiency virus type 1 isolates have a lower level of pathogenic fitness than other dominant group M subtypes: implications for the epidemic. *J. Virol.* **83**, 5592–605 (2009).
82. Ball, S. C. *et al.* Comparing the ex vivo fitness of CCR5-tropic human immunodeficiency virus type 1 isolates of subtypes B and C. *J. Virol.* **77**, 1021–38 (2003).
83. Quinones-Mateu, M. E. *et al.* A Dual Infection/Competition Assay Shows a Correlation between Ex Vivo Human Immunodeficiency Virus Type 1 Fitness and Disease Progression. *J. Virol.* **74**, 9222–9233 (2000).
84. Lassen, K. G. *et al.* Elite suppressor-derived HIV-1 envelope glycoproteins exhibit reduced entry efficiency and kinetics. *PLoS Pathog.* **5**, e1000377 (2009).
85. Ball, S. C. *et al.* Comparing the Ex Vivo Fitness of CCR5-Tropic Human Immunodeficiency Virus Type 1 Isolates of Subtypes B and C. *J. Virol.* **77**, 1021–1038 (2003).
86. King, D. F. L. *et al.* Mucosal tissue tropism and dissemination of HIV-1 subtype B acute envelope-expressing chimeric virus. *J. Virol.* **87**, 890–9 (2013).
87. Ariën, K. K., Vanham, G. & Arts, E. J. Is HIV-1 evolving to a less virulent form in humans? *Nat. Rev. Microbiol.* **5**, 141–151 (2007).
88. Martinez-Picado, J. *et al.* Fitness Cost of Escape Mutations in p24 Gag in Association with Control of Human Immunodeficiency Virus Type 1. *J. Virol.* **80**, 3617–3623 (2006).
89. Ariën, K. K. *et al.* The replicative fitness of primary human immunodeficiency virus type 1 (HIV-1) group M, HIV-1 group O, and HIV-2 isolates. *J. Virol.* **79**, 8979–90 (2005).

90. Venner, C. M. *et al.* Infecting HIV-1 Subtype Predicts Disease Progression in Women of Sub-Saharan Africa. *EBioMedicine* **13**, 305–314 (2016).
91. Leite, T. C. N. F. *et al.* Impact of HIV-1 Subtypes on AIDS Progression in a Brazilian Cohort. *AIDS Res. Hum. Retroviruses* **33**, 41–48 (2017).
92. Amornkul, P. N. *et al.* Disease progression by infecting HIV-1 subtype in a seroconverter cohort in sub-Saharan Africa. *AIDS* **27**, 2775–2786 (2013).
93. Kiwanuka, N. *et al.* HIV-1 subtypes and differences in heterosexual HIV transmission among HIV-discordant couples in Rakai, Uganda. *AIDS* **23**, 2479–84 (2009).
94. Kahle, E. *et al.* HIV-1 subtype C is not associated with higher risk of heterosexual HIV-1 transmission. *AIDS* **28**, 235–243 (2014).
95. Morrison, C. S. *et al.* Hormonal contraception and the risk of HIV acquisition. *AIDS* **21**, 85–95 (2007).
96. Morrison, C. S. *et al.* Plasma and cervical viral loads among Ugandan and Zimbabwean women during acute and early HIV-1 infection. *AIDS* **24**, 573–82 (2010).
97. Morrison, C. S. *et al.* Hormonal contraceptive use and HIV disease progression among women in Uganda and Zimbabwe. *J. Acquir. Immune Defic. Syndr.* **57**, 157–64 (2011).
98. Lemonovich, T. L. *et al.* Differences in Clinical Manifestations of Acute and Early HIV-1 Infection between HIV-1 Subtypes in African Women. *J. Int. Assoc. Provid. AIDS Care* **14**, 415–422 (2015).
99. Dudley, D. M. *et al.* A novel yeast-based recombination method to clone and propagate diverse HIV-1 isolates. *Biotechniques* **46**, 458–467 (2009).
100. REED, L. J. & MUENCH, H. A SIMPLE METHOD OF ESTIMATING FIFTY PER CENT ENDPOINTS¹². *Am. J. Epidemiol.* **27**, 493–497 (1938).
101. Gao, Y. *et al.* Calculating HIV-1 Infectious Titre Using a Virtual TCID₅₀ Method. in 27–35 (Humana Press, 2008). doi:10.1007/978-1-59745-170-3_3
102. Marozsan, A. J. *et al.* Relationships between infectious titer, capsid protein levels, and reverse transcriptase activities of diverse human immunodeficiency virus type 1 isolates. *J. Virol.* **78**, 11130–41 (2004).
103. Torre, V. S. *et al.* Variable sensitivity of CCR5-tropic human immunodeficiency virus type 1 isolates to inhibition by RANTES analogs. *J. Virol.* **74**, 4868–76 (2000).
104. Kumar, S., Stecher, G., Li, M., Knyaz, C. & Tamura, K. MEGA X: Molecular evolutionary genetics analysis across computing platforms. *Mol. Biol. Evol.* **35**, 1547–1549 (2018).
105. NDRI. Available at: <https://ndriresource.org/>. (Accessed: 20th June 2019)
106. Hathaway, N. J., Parobek, C. M., Juliano, J. J. & Bailey, J. A. SeekDeep: single-base resolution de novo clustering for amplicon deep sequencing. *Nucleic Acids Res.* **46**, e21–e21 (2018).
107. Klein, Katja; Nankya, Immaculate; Nickel, Gabrielle; Ratcliff, Annette N.; Meadows, Adam A.J.; Hathaway, Nicholas; Bailey, Jeffery A.; Stieh, Daniel J.; Cheeseman, Hannah; Carias, Ann M.; Lobritz, Michael A.; Mann, Jamie F.S.; Gao, Yong; Hope, Thomas J.; E. J. Acute envelope chimeric HIV-1 show higher transmission fitness across primary human mucosal tissues compared to chronic

- envelope chimeric variants (Submitted to Plos Pathogens). *PLoS Pathog.* (2019).
108. Silvestri, G., Paiardini, M., Pandrea, I., Lederman, M. M. & Sodora, D. L. Understanding the benign nature of SIV infection in natural hosts. *J. Clin. Invest.* **117**, 3148–3154 (2007).
 109. VandeWoude, S. & Apetrei, C. Going wild: lessons from naturally occurring T-lymphotropic lentiviruses. *Clin. Microbiol. Rev.* **19**, 728–62 (2006).

Curriculum Vitae

SPENCER YEUNG

EDUCATION

University of Western Ontario (Western University), London, ON <i>Master of Science (MSc)</i>	2017-2019
<ul style="list-style-type: none">Specialization in Microbiology and Immunology	
<i>Master of Management of Applied Science (MMASc)</i>	2016- 2017
<ul style="list-style-type: none">Specialization in Global Health Systems	
Bachelor of Medical Sciences (BMSc)	2012-2016
<ul style="list-style-type: none">Honours Specialization in Physiology	

RESEARCH EXPERIENCE

Department of Microbiology and Immunology, UWO, London, ON <i>MSc Candidate</i>	2017-2019
<ul style="list-style-type: none">Thesis: Determining the Relative Transmission Fitness of HIV-1 Subtypes A, B, C, and DResearch Advisor: Dr. Jessica Prodger and Dr. Eric Arts	
Rakai Health Sciences Program, Kalisizo, Uganda <i>Research Student</i>	2017
<ul style="list-style-type: none">PBMC isolation for HIV-1 cure studiesResearch Advisor: Taddeo Kityamuweesi and Dr. Jessica Prodger	
Department of Medicine, UWO, London, ON <i>Thesis Student</i>	2015-2016
<ul style="list-style-type: none">Thesis: Using Next-Generation Sequencing to find genetic variants associated with cisplatin-induced ototoxicityResearch Advisor: Dr. Wendy Teft and Dr. Richard Kim	
Department of Communication Sciences and Disorders, UWO, London, ON <i>Research Assistant</i>	2015
<ul style="list-style-type: none">EEG tests on children aged 4-10 with typical or autism spectrum language developmentResearch Advisor: Dr. Janis Cardy	

ACADEMIC HONOURS AND AWARDS

Queen Elizabeth II Diamond Jubilee Scholarship	2016-2017
Dean's Honour List	2012-2016
Western Scholarship of Excellence	2012-2013

VOLUNTEER ACTIVITIES AND EXPERIENCE

MNI Social Committee	2018-2019
MMASC Representative 2017	2016-2017